KERNFORSCHUNGSANLAGE JÜLICH
GESELLSCHAFT MIT BESCHRÄNKTER HAFTUNG
BR9024505

NUCLEBRÁS
Empresas Nucleares Brasileiras SA

NUCLEBRAS/CDTN 424/80
(HBK-IB-2/80)

TH-UTILIZATION IN PRESSURIZED WATER REACTORS

TASK 1. - STATUS OF KNOWLEDGE - $(Th,U)O_2$-USE IN WATER REACTORS STATUS REPORT.

NUCLEBRAS
KFA
KWU
NUKEM

CDTN -- 424/80 (HBK - IB - 2 /80)

MARCH 1980

CONTENTS

		Page
1.	Manufacturing techniques	1
1.1	Kernel fabrication	1
1.1.1	Process description	1
1.1.2	Advantageous features of the gel-precipitation process	2
1.2	Pellet fabrication of standard UO_2	3
1.2.1	The AUC process	3
1.2.2	The direct pelletizing process	4
1.2.3	Advantageous features of the UO_2 ex AUC technology	4
1.3	Experiences in manufacturing of $(Th,U)O_2$-fuel under the D_2O-Th-program	5
1.3.1	Kernel fabrication	6
1.3.2	Vibratoriliy compaction and fuel rod fabrication	7
1.3.3	Pellet fabrication	8
2.	Characterization of $(Th,U)O_2$-fuel (methods, equipment, results)	17
2.1	Chemical Analysis	17
2.1.2	Analysis of Uranium Isotopes	17
2.1.2	Uranium and Thorium Analysis	17
2.1.3	Impurity Analysis	18
2.2	Determination of O/M-ratio and the total amount of U in $(Th,U)O_2$-fuel	20
2.3	Structural analysis	21
2.4	Physical properties	21
2.4.1	Density and porosity	21
2.4.2	Thermal conductivity	22
2.4.3	Specific surface area	22
2.4.4	Solid phase analysis	23
3.	Performance	30
3.1	Description of the former D_2O-Th-program	30
3.1.1	Investigations on sol-gel derived $(Th,U)O_2$-kernels	30
3.1.2	Investigations on kernel batch properties	30
3.1.3	Objective of the irradiation program	31
3.2	Experimental techniques	31
3.3	Irradiation history	32
3.4	Post-irradiation examination results	33

		Page
3.4.1	Structure of irradiated fuel	33
3.4.2	Uranium-distribution within the fuel rod	34
3.4.3	Fission gas release	34
3.4.4	Cycling behavior of the fuel	35
3.4.5	Defects	35
3.5	Reprocessing	36
3.6	Evaluation	36
4.	Literature review on performance	48
4.1	Fabrication processes	48
4.1.1	Pelletizing process	48
4.1.2	Vi-pac process	49
4.1.3	Sphere-pac process	49
4.1.4	Extrusion process	49
4.1.5	Properties	50
4.2	Irradiation testing	50
4.2.1	$(Th,U)O_2$-fuel performance in test reactors	50
4.2.2	$(Th,U)O_2$-fuel element performance in power reactors	53
4.2.3	$(Th,Pu)O_2$-fuel performance	55
5.	Review of direct pelletizing with ex-gel $(Th,U)O_2$-fuel and impact on the program	66
5.1	Pressfit powder properties	66
5.2	Sinterfit powder properties	67
5.3	Summary	68
6.	Status report on Brazilian expertise	69
6.1	Introduction	69
6.2	Methods and equipments	70
6.2.1	Zircaloy tubes and bars	70
6.2.2	Uranium oxide (UO_2) pellets	70
6.2.3	Machining and dimensional control of tubes and endplugs	72
6.2.4	Cleaning of tubes and plugs	73
6.2.5	Welding of the first endplug to the tube	73
6.2.6	Quality control of the first weld	73
6.2.7	Loading of the UO_2 pellets	74
6.2.8	Welding of the second endplug to the rod	75
6.2.9	Sealing of the second plug	76
6.2.10	Rod quality control	76

1. Manufacturing techniques

1.1 Kernel fabrication

For the preparation of spherical particles, powder and wet-chemical processes can be employed. Wet-chemical processes have proven to be very suitable for the production of fuel kernels for High Temperature Reactor fuel elements. A special wet-chemical process using the gelprecipitation has been developed at NUKEM/HOBEG up to the production scale, according to which all current types of spherical nuclear mixed-oxide, feed and breed particles (mostly called kernels), containing high melting uranium and thorium oxides or carbides, respectively, can be fabricated by only slight changes in the composition of the feed solution and of some process parameters. Table 1.1 demonstrates the kernel types, their main properties and the produced quantity. The diameter of the kernels is within the range of 200 to 800 /um, the mixture ratio of ThO_2:UO_2 is between 4:1 and 40:1. The widest experience is based on the production of mixed-oxide kernels with 400/um diameter for the nuclear reactors AVR and THTR-300 within a production line of 18 kg $(Th,U)O_2$-kernels daily throughput. The production line operates since 1973 and achieves more than 95 % yield at a narrow grain size distribution and a standard deviation of the mean diameter of generally 4 % or less.

1.1.1 Process description

The gel-precipitation process for ThO_2, UO_2 and mixed-oxide kernels is presented in a flow sheet in Fig. 1.1.

For production of mixed-oxide kernels, solutions of uranyl nitrate, thorium nitrate and an aqueous solution of polyvinyl alcohol (PVA) as auxiliary material are homogeneously mixed in a specified ratio. Using mechanical vibration of an electromagnetic vibration system this feed solution is passed through nozzles, generating jets of liquid in air which disperse into uniform droplets. The droplets are solidified by reaction with ammonia gas and are collected in ammonia solution. Subsequently, the spherical particles are purified from the by-product ammonium nitrate with aqueous ammonia and are dehydrated with isopropanol. Drying is performed by low-pressure distillation at 500 mbar, thereby recovering isopropanol. The dried particles are calcined in air at 300°C, whereby the thorium oxide hydrate is dehydrated and the ammonium diuranate and the

PVA are thermally decomposed. The kernels are sintered in H_2-atmosphere to $(Th,U)O_2$-mixed-oxide of 97 to 99 % of the theoretical density. The throughput in the production facility is 4 kg of heavy metal per hour.

Further development led to an essential simplification of the process steps washing, drying, and calcination. In slightly alterating the feed solution composition, it is possible to wash the kernels with water instead of isopropanol and maintain the same quality. The change-over of the process to water washing results in the following process simplifications:

- measures of fire and explosion protection can be omitted, as no burnable materials are used;
- the waste problem is simplified by the abolition of isopropanol recycling.

1.1.2 Advantageous features of the gel-precipitation process

The advantages of the gel-precipitation process are characterized by

- great flexibility in the composition of the feed solution;
- chemical stability of the feed solution;
- simple droplet formation and narrow grain spectrum;
- high throughput and yield;
- high kernel density;
- simple waste treatment;
- profound technical know-how.

Special characteristics of the gel-precipitation process are:

- The feed solution is a clear liquid, the stability of which is nearly unlimited, even at room temperature thereby allowing exact volume dosage (flow meters) being necessary for the adjustment of defined kernel sizes; precipitations do not occur. In contrast to other processes, no clogging of the sphere formation equipment (tank, tubes or pipes, nozzles, etc.) occurs by instantaneous or slow hardening of the feed solution. In practical operation, feed solution residues are recycled in the next charge.

- The sphere formation conditions, such as uranium and thorium concentration, viscosity, temperature, can largely be adapted to the demanded kernel size; soluble and solid substances can be added within a wide range.

- The ammonia solution used for sphere formation and washing can be handled in the usual industrial way and does not need a special CO_2-purification. No formation of soluble carbonate complexes of uranium has been observed. Therefore, reprocessing of the washing filtrate for recovery of uranium and thorium can be omitted completely.

- Uniform and high dense kernels are obtained already at low sinter temperatures of 1100°C due to the good sintering behavior of the intermediate products.

- As waste, only ammonium nitrate is produced during neutralization of uranium and thorium nitrates with ammonia.

- At present, a procedure for ammonium nitrate disposal is being developed. The auxiliary materials NH_3 and isopropanol can be recycled.

1.2 Pellet fabrication of standard UO_2

The fabrication of UO_2 pellets from the feed material uraniumhexafluoride (UF_6) and aqueous solutions of Uranylnitratehydrate (UNH) consists of two processing areas: (1) The production of UO_2 powder by a chemical process, called conversion; (2) The fabrication of UO_2 pellets from UO_2 powder by powder metallurgical methods, called pelletizing.

For the conversion there are three alternatives of industrial manufacturing processes. There are two wet conversion processes, where intermediate products are precipitated from aqueous solutions. The uranium compounds are ammonium diuranate (ADU) or ammonium uranyl carbonate (AUC). The third process is the dry conversion process, where UF_6 is directly processed into UO_2 powder. The latter process can only start with the feed material UF_6 whereas the wet conversion processes can start either with UF_6 or UNH.

There are also three alternatives for the pelletizing which are combined with the distinct conversion processes. These are dry granulation or prepressing method with ex-ADU and ex-dry-conversion powder. The third process is direct pelletizing with ex-AUC powder. In this process no intermediate product during the pelletizing step, no granulate is necessary. It is also the direct pelletizing process into which scrap recycling (U_3O_8) can easely be integrated.

At KWU/RBU, the UO_2 powder is produced by the AUC conversion route, and consequently the direct pelletizing process is applied for pellet production.

1.2.1 The AUC process

The main features of the AUC conversion are shown in the flow sheet of Fig. 1.2.

The first step is the evaporation of UF_6. Secondly, the precipitation of the AUC powder. UF_6 (or UNH), CO_2 and NH_3 are fed into the precipitator. The AUC precipitates in the form of yellow single crystals, the grain size of which depends on the precipitation parameter, for example the temperature and the P_H value.

The third step is the filtration of the suspension on a vacuum filter and the subsequent washing with ammonium carbonate and methylalcohol. The AUC is a very well defined uranium compund with a very low fluorine content, typically less than 300 ppm.

The next step is the calcination and reduction step, in a fluidized be furnace. The carrier gas is hydrogen and steam. The treatment of the powder is sufficiently smooth and usually conserves the shape and identity of the particles. A pyrohydrolysis step, integrated into the fluidized bed process, lowers the fluorine content of the UO_2 powder to very low values, e.g. less than 60 ppm.

The UO_2 powder is pneumatically transported into the homogenizer, a rotating mixer blender, wherein about 2000 kg are softly treated without influencing the powder properties. During this step, U_3O_8 from dry recycled material (oxidized rejected UO_2 pellets), is mixed with fresh UO_2 powder.

1.2.2 The direct pelletizing process

The flowability of the UO_2 powder permits a high throughput by the use of multi-die or rotarting presses. The powder is directly pressed without any treatment (milling, prepressing, granulating e.g.) and without the addition of any organic materials as binder, lubricant or pore former. So, there's no need of a dewaxing step before sintering, pellets are sintered directly. The green pellets fabricated by the direct pelletizing process are perfect with respect to their surface condition and microstructure and show a high strength. They are sintered at about 1700°C in hydrogen. The sintered and centerless ground pellets also show excellent surface conditions and fulfill a tight specification regarding physical, chemical and microstructural properties.

1.2.3 Advantageous features of the UO_2 ex AUC Technology

To summarize the characteristic features of the UO_2 ex AUC pellet technology, three major groups of advantages are to be considered: 1) "Wet conversion", 2) "dry scrap recycling" and 3) "direct pelletizing".

1) Wet conversion means: (Fig. 1.3)

- UNH can be fed into the AUC precipitator instead of UF_6. The use of UNH is important for natural uranium fuel e.g. for heavy water reactors UO_2-PuO_2 mixed-oxide fuel, processing of reprocessed spent fuel and wet blending.
- The powders, AUC as well as UO_2 are free flowing and can be pneumatically transported. The UO_2 powder shows good blending behaviour and can be used in a direct pelletizing process.
- At least: The direct control of pellet properties with respect to chemical purity, density and microstructure is possible. The basis for "direct control of pellet properties" is the fact that usually one AUC crystal becomes one UO_2 particles which becomes one UO_2 grain in the final UO_2 pellet.

2) Dry scrap recycling (Fig. 1.4)

is a method to further control the pellet properties. U_3O_8 additions to the UO_2 powder decrease the sintered density of the pellets. Therefore, the pellet density can be controlled with constant pressing and sintering parameters.

UO_2 pellets from the AUC powder process have a homogeneous pore structure (randomly spaced pores) as compared to a granulate structure. Pellets with homogeneous microstructure show less pellet defects, e.g. chips, cracks. U_3O_8 additions automatically generate pores with a size which is optimized with respect to compensation for fission-induced swelling and densification. Dry scrap recycling is a very economic method of recycling fabrication returns.

3) The direct pelletizing process (Fig. 1.5) means:

Only UO_2 and U_3O_8 are feed material for pelletizing. There is no binder, lubricant and pore former added to the powder.

Direct pelletizing means "direct pressing" without milling, prepressing, granulating, and "direct sintering" without a dewaxing step.

1.3 Experiences in manufacturing of $(Th,U)O_2$-fuel under the D_2O-Th-Program

Within the R & D-program "Development of D_2O-moderated and cooled Breeder Reactor", a fuel rod was designed according to the requirements containing sol-gel derived vibratorily compacted $(Th,U)O_2$-fuel within a Zircaloy-4 cladding.

1.3.1 Kernel fabrication

The development of processes for the fabrication of fuel rods for the D_2O-Th-Breeder Reactor using high-dense spherical $(Th,U)O_2$-particles (kernels) was concentrated on the sol-gel process. This used sol-gel process is based on the internal gelation of Th/U-sol droplets in manufacturing kernels with a mixture ratio of ThO_2 to UO_2 of about 40:1. The process comprises three steps:

- preparation of the Th/U-sol
- sphere formation by dispersion of the sol into a water-insoluble organic liquid and gelation of the droplets
- drying of the gelled spheres and calcining/sintering to mixed-oxide kernels.

Sol-preparation

Thorium nitrate solution is mixed with uranyl nitrate solution in a specified ration and subsequently precipitated with ammonium hydroxide at 50°C. After adding nitric acid, the freshly precipitated thorium hydroxide-ammonium diuranate mixture is peptized at temperatures between 90 and 95°C. The NO_3^-/Th+U ratio is adjusted to between 0.3 and 0.4. Then the sol is partially evaporated under vacuum in order to reach a concentration of 4 to 6 mole Th+U per liter.

Sphere formation and gelation

The sol is mixed with a solution of hexamethylene-tetramine at room temperature. Fabrication of microspheres is performed by dropping into an water-insoluble organic liquid, preferably paraffin oil, at 90 to 95°C. According to surface tension, droplets form, which solidify to a gel at increased temperatures. Decomposition of hexamethylene-tetramine causes internal gelation of the droplets. To produce smaller microspheres, the solution is passed into the oil through a binary nozzle with an orifice diameter of 0.5 mm. The oil adhering to the microspheres is removed by washing (2 - 3 hours) with carbon tetrachloride in a Soxhlet-apparatus. Subsequently, still present NO_3-ions are washed out with ammonium hydroxide.

Drying, calcining and sintering

The microspheres are dried in an apparatus with perforated bottom in flowing warm air within 2 hours. In preliminary tests the dried kernels were heated in a drying oven up to 300°C and then calcined in a muffle furnace at 800°C respectively 1000°C. Later on, calcining was performed in a tube

furnace which is heated from 20° to 1000°C in a course of several hours. In a horizontal tube furnace 500 g kernels are calcined in alumina boats, in contrast to a vertical tube furnace (20 cm bed height) producing 2 kg calcined kernels. After calcining, the kernels are sintered in a sintering furnace at 1600°C to 1700°C in hydrogen atmosphere.

1.3.2 Vibratorily compaction and fuel rod fabrication

To obtain a sol-gel derived compacted fuel rod the kernels can be vibrated into the cladding tube by three different kinds of methods:

- A homogeneous mixture from kernels with adequate size distribution is prepared, filled by a conveyer system into the cladding tube and then compacted by vibration.
- By different conveyers, the individual kernel fractions are simultaneously filled into the cladding tube, being controlled to achieve a homogeneous kernel size distribution all over the fuel column. Finally, the kernel loose packing is compacted by vibration.
- The kernel fractions are packed into the tube by an infiltration method, i.e. the large kernels are filled into the cladding and compacted to its maximum attainable density; afterwards the kernels with the finer diameters are infiltrated into the remaining void volumes by low vibration.

Investigations of these different methods resulted in giving the last method the priority because this method attains the highest fuel density, the lowest density variation and the shortest infiltration periods.

Investigating the different vibration parameters, e.g. frequency and acceleration showed that a frequency of 50 Hz and an acceleration of 10 g resulted in the highest densities. Thus the requirements on the vibration system are low and the vibration procedures are quite simple.

Besides the density of the fuel column the infiltration time is of great interest. The design of the screen and the proportion of the kernel diameter of each fraction are of great influence on the infiltration time. An adequate experimental optimization of the screen may reduce the infiltration time by a factor to 10. When filling the large kernel fraction into a 2500 mm long fuel rod, the compaction time is 5 minutes, and another 60 minutes for infiltrating the fine fraction. The infiltration velocity was 40 mm/min. Typical results of vibration testing with tubes of 10.5 mm inner diameter are summarized in Table 1.2.

To demonstrate the developed technology, two test rods of about 2500 mm length were manufactured, inspected and examined, showing noproblems as mentioned above. The fuel rod had fission gas plena at both ends, so the air had been evacuated through the fuel column. Evacuation and filling time were performed within 105 minutes. All other manufacturing steps of the test rods could be performed in the usual manner. Table 1.3 summarizes the most essential data from the prototype manufacturing.

1.3.3 Pellet fabrication

Within the D_2O-Th-program, in addition to the fabrication of vibratorily compacted mixed-oxide fuel, 250 kg $(Th,U)O_2$-fuel was manufactured in 1964. The fuel was needed to perform a critical experiment. The fuel consists of pellets having the dimensions of 10.0 ± 0.1 mm in diameter and with a heavy metal composition of 97,5 % ThO_2 and 2.5 % UO_2. The uranium was 93 %-enriched U-235. The specified pellet density was 8.8 ± 0.2 g/cm^3.

The fuel was manufactured in the normal production lines for UO_2. The fabrication process comprised the steps powder mixing, pressing and sintering in hydrogen-atmosphere. The defined specifications could be reached. However, the homogeneity, the structure and the geometrical shape were inadequate under the aspect of using this fuel as reactor fuel. Nevertheless, the manufactured fuel could be used because it was only applied to a critical experiment.

kernel type	Th/U ratio	diameter (/um)	produced quantity (kg)
$(Th,U)O_2$	40:1 to 4:1	200, 400, 500, 600 and 800	> 10.000
ThO_2		400, 500, 600	> 3.000
UO_2		200, 300	about 100
UC_2		200	> 100
U-C-O		200, 300	about 200

Table 1.1: Types and quantities of fabricated kernels

Nr.	ID cladding D (mm)	particles Ø coarse fraction d_1 (µm)	particles Ø fine fraction d_2 (µm)	D/d_2	d_1/d_2	W/O of fine fraction d_2 (mm)	fuel length (mm)	Density % fraction	Density % complete fuel	Smeared density (% th. D.?)
1	10,5	300 - 400	-	29	-	-	400	63,7	-	-
2	10,5	300 - 400	33 - 80	29	6	24,1	400	-	83,0	80,2
3	10,5	400 - 500	-	22	7,5	-	400	63,2	-	-
4	10,5	400 - 500	33 - 80	22	7,5	22,7	400	-	81,7	79,8
5	10,5	500 - 630	-	18	-	-	400	63,9	-	-
6	10,5	500 - 630	33 - 80	18	10	24,2	400	-	83,6	80,7
7	10,5	630 - 750	-	14	-	-	400	64,2	-	-
8	10,5	630 - 750	33 - 80	14	12	24,8	400	-	84,7	81,8
9	10,5	750 - 1000	-	11	-	-	400	64,3	-	-
10	10,5	750 - 1000	33 - 80	11	15	25,4	400	-	85,0	82,2
11	10,5	500 - 750	-	16	-	-	400	64,5	-	-
12	10,5	500 - 750	33 - 80	16	11	24,2	400	-	84,4	81,5
13	10,5	630 - 1000	-	12	-	-	400	63,6	-	-
14	10,5	630 - 1000	33 - 80	12	14	24,6	400	-	84,7	82,1
15	10,5	500 - 750	33 - 100	16	9,5	23,6	400	-	83,6	80,8
16	10,5	630 - 750	33 - 100	14	10	24,6	400	-	84,3	81,5
17	10,5	630 - 1000	33 - 100	12	12	24,6	400	-	84,8	82,0
M 1+	10,5	630 - 1000	33 - 100	12	12	23,5	2328	-	83,2	80,4
M 2+	10,5	630 - 1000	33 - 100	12	12	24,4	2328	-	84,8	82,0

+ Musterstäbe

Table 1.2: Characteristic results from vibration-compactions investigations with spherical $(Th,U)O_2$-fuel

		M 1	M 2	Observation
fuel		$(Th,U)O_2$-particles		
coarse fraction	(/um)	630 - 1000		
fine fraction	(/um)	33 - 100		
water content	(ppm)	16 coarse fraction 16 fine fraction		analysed after Vibro-Compaction
gas content	(Nml/g)	0,012 0,011		coarse fraction fine fraction
particle mass rod	(g)	1646	1676	
coarse particle rod	(g)	1259,5	1267	
fine particle rod	(g)	386,5	409	
full length	(mm)	2328 $\pm$ 0,5	2328 $\pm$ 0,5	
average density	(% th.D.)	80,4	82,0	
density variation	(% th.D.)	max $^{+1,6}_{-3,0}$	max $^{+2,4}_{-2,1}$	
x-ray first end cup		o.k.	o.k.	
x-ray second end cup		o.k.	o.k.	
leak rate	(mbar l/sec.)	$< 10^{-8}$	$< 10^{-8}$	

Table 1.3: Characteristic data from the investigation of prototypical fuel rods with vibratorily-compacted-fuel

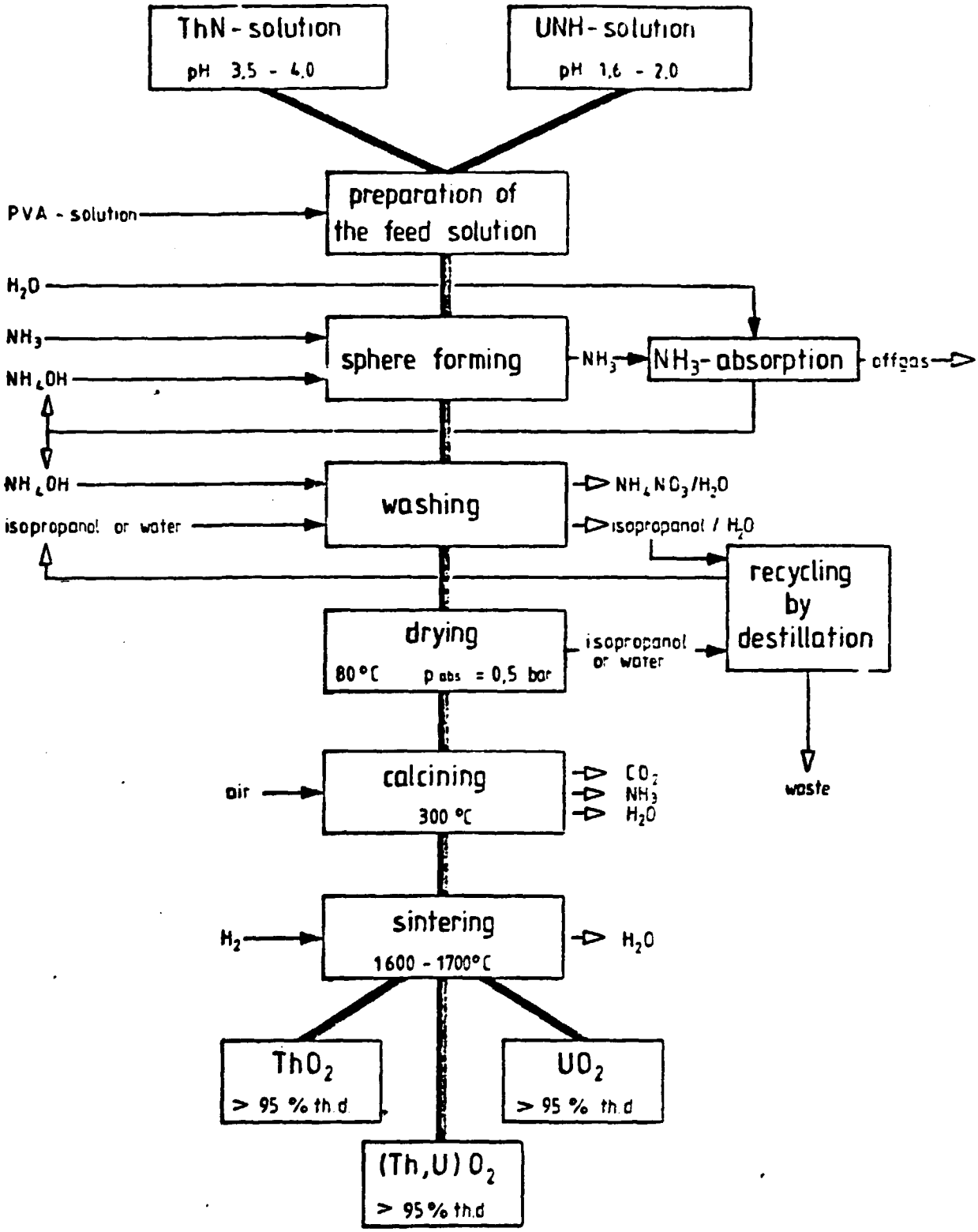

Fig. 1.1: Flowsheet of the gel-precipitation process for the fabrication of ThO_2, UO_2 and mixed oxid kernels.

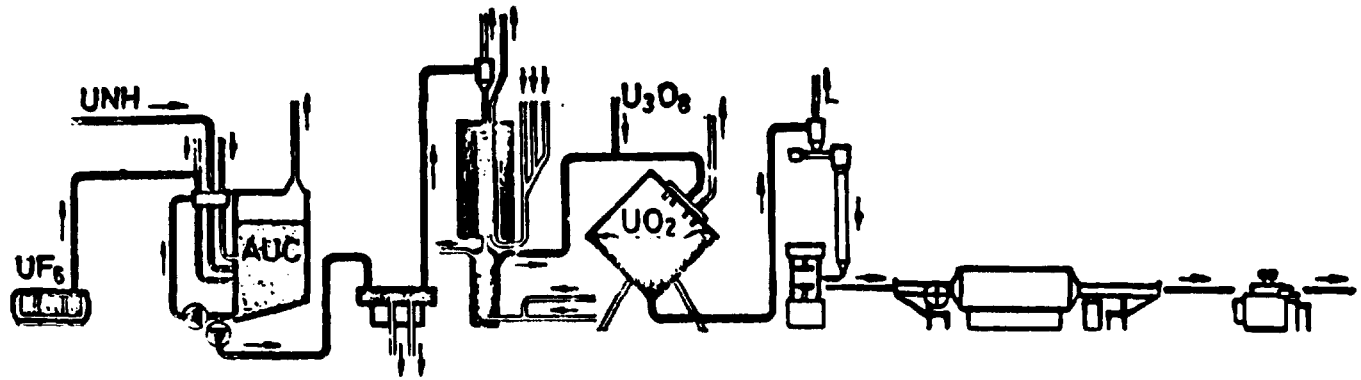

Fig. 1.2: AUC conversion and pelletizing process

FEED MATERIAL UNH

Natural uranium fuel

UO_2-PuO_2 recycle fuel

Reprocessed spent fuel

Wet blending

FLOWABILITY OF POWDERS

Pneumatic transport

Good blending

Direct pelletizing

DIRECT CONTROL OF PELLET PROPERTIES

Chemical purity

Density and microstructure

Fig. 1.3: Features of the AUC powder technology

CONTROL OF PELLET PROPERTIES

Density (constant pressing and sintering parameters)

Homogeneous pore structure

Optimized pore size

ECONOMIC SCRAP RECYCLING

HIGH SURFACE QUALITY STANDARD

Fig. 1.4: Features of the AUC powder technology

FEED MATERIAL = URANIUM OXIDE

No binder

No lubricant

No pore former

Only U_3O_8 addition

DIRECT PRESSING

No milling

No prepressing

No granulating

DIRECT SINTERING

No dewaxing

ADAPTABILITY TO ADVANCED PROCESSES

Low temperature sintering

Sintering to size

Fig. 1.5: Features of the AUC powder technology

2. Characterization of $(Th,U)O_2$-fuel (methods, equipment, results)

Methods to investigate $(Th,U)O_2$-fuel had to be provided for testing the designed specifications of the fuel.

2.1 Chemical Analysis

In order to characterize kernels a number of test methods are applied. The chemical methods of analysis are specified in the following.

2.1.1 Analysis of Uranium Isotopes

$(Th,U)O_2$-kernels are dissolved in a HNO_3/HF mixture. From this solution thorium is precipitated in form of oxalate, the filtrate is evaporated and fired. The fire residue is dissolved in HNO_3 and is analysed as to the portions of U-234, U-235, U-236 and U-238 by means of a mass spectrometer. The results are stored on a punched tape and evaluated in a computer by means of the Fortran-Programme DAIS∅. Measuring accuracy amounts to 0,1 % for high enriched U-235.

2.1.2 Uranium and Thorium Analysis

1 g of $(Th,U)O_2$-kernels is treated with 20 ml of HNO_3/HF mixture. The solution is concentrated by evaporation to about 5 ml, diluted with water to 100 ml; thorium precipitated as oxalate with 30 ml of saturated oxalic acid solution at 80°C. The precipitate is digested overnight, filtered, washed, dried, calcined at 1100°C for 4 hours to stoichiometric ThO_2 and weighed.

The filtrate of the oxalate precipitation is evaporated to dryness and calcined at 600°C in order to destroy completely the organic compound. The remaining residue is dissolved using HNO_3. For determination of uranium the solution is concentrated by evaporation; uranium (VI) is reduced in phosphoric acid medium in the presence of aminosulphonic acidby excess of Fe (II) sulphate to U (IV). The excess of Fe (II) is then selectively oxidized with nitric acid in the presence of molybdenum (VI) as catalyst. After addition of 1 M sulphuric acid and vanadyl sulphate crystals, the uranium content is determined potentiometrically by titration with 0,027 N potassium dichromate solution. The error of thorium and uranium analysis is $\pm$ 0.1 % for each element.

2.1.3 Impurity Analysis

The concentration of impurities in a ppm-range is determined according to the following methods;

- Em, emission spectrographic method - no pre-concentration of impurities
- Cem, emission spectrographic method where a chemical enrichment process was used for the pre-concentration of impurities prior to the spectrographic analysis
- AAS, atomic absorption spectrophotometry methods
- Phot, spectrophotometric methods.

Emission Spectrographic Analysis (Em)

For spectroscopic analysis the powdered kernels are fired for 1 hour at 800°C.

According to the carrier distillation method, the elements Ag, Al, B, Ba, Be, Bi, Ca, Cd, Co, Cr, Cu, Fe, In, Mg, Mn, Mo, Na, Ni, P, Pb, Si, Sn, V and Zn are determined by means of 2 % Ga_2O_3 as carrier.

Al, Fe, Mg and Mn are evaluated with regard to the internal standard Cr_2O_3, the other elements are evaluated directly. The advantage of the emission spectrographic analysis in accordance with the carrier distillation principle is, that relatively many elements can be determined at the same time. However, the total impurity rate must not exceed a certain limit, as matrix effects falsify the analysis to a large extent. Apart from the matrix effects already mentioned, further disadvantages of this analysis are, that exactitude mostly lies only between 10 - 30 % and the detection efficiency for some specified elements (e.g. Ba, Ca, V) often is not sufficient. In such a case, some elements are determined by means of atomic absorption spectrometry (AAS) or spectrophotometrically (Phot).

Emission Spectrographic Method (Cem)

A number of elements, the rare earths, and the elements of stable oxides such as V, W, Ti, Zr, Hf, Nb and Ta are determined by means of the enrichment method which consists of chemical separation and emission spectrographical final determination.

The elements Hf, Nb, Sb, Sn, Ta, Ti, V, W and Zr are separated from uranium by Cupferron extraction with $CHCl_3$. After addition of Ga_2O_3 as internal standard the residue is fired at 500°C and, subsequently, after adding Li_2CO_3, is determined spectrographically in a direct current arc in argon oxygen atmosphere.

After adding Y as precipitation partner, rare earths (RE) are precipitated in form of RE-fluorides from nitric uranium solution with HF. The filtered RE-fluorides are mixed with Li_2CO_3 and are determined spectrographically in argon oxygen atmosphere.

Atomic Absorption Spectrophotometry analysis (AAS)

The elements Ag, Cd, Co, Cr, Cu, Fe, K, Li, Mg, Mn, Na, Ni and Zn were determined after separation of uranium with TBP/hexanextraction according to the AAS method. Calibration is carried out with synthetical samples.

For quick operational analysis the elements Ca and Na were calibrated without separating uranium beforehand. However, the calibration curve shows a flatter slope.

Spectrophotometry (Phot)

As an alternative method for determination or supplementation to AAS, respectively, some impurities are determined spectrophotometrically according to known methods.

In a nitric medium chromium (VI) forms with diphenyl carbazide a reddish-violet complex, the colour intensity of which is measured at 530 µm.

After reduction of Fe (III) to Fe (II) by means of hydroxylaminhydrochloride, the colour turns to red when 1,10-phenanthroline is added. The extinction is measured at 530 µm.

In the presence of traces of Cu, Co, Cr, Fe and other impurities Ni, in form of a Ni (II)-dimethylglyoxim complex, can be separated from uranium in an alkaline medium by chloroform. By adding ammonium citrate uranium is kept in solution. Extinction of the Ni (II)-dimethylglyoxim complex is measured at 450 µm.

Copper is separated from uranium by means of chloroform extraction. By adding ammonium Cu is separated from the chloroform phase and is mixed with Na-diethyldithiocarbamat. The Cu-complex dissolves in CCl_4 and is also measured photometrically at 450 µm in this medium.

As is separated from uranium in form of $AsCl_3$ by means of extraction with $CHCe_3$ and, subsequently, is determined photometrically according to the Mo-blue method.

2.2 Determination of O/M-ratio and the total amount of U in $(Th,U)O_2$-fuel

The most simpliest and most exact method to determine as well the O/M-ratio as the U-content of a $(Th,U)O_2$-fuel is the controlled potential coulometry. The method is based on the fact that Th(IV)-ions are extremely stable in a solution while the valency of uranium can be easily changed from the U(IV) to the U(VI) state. Thus small amounts of uranium can be detected in solution with a greater amount of thoriumm as the stability of the Th(IV) valence state changes in the O/M-ratio of a $(Th,U)O_{2 \pm x}$ fuel is only attributed to the uranium ions in the lattice. When $(Th,)O_2$ of exactly stoichiometric composition is dissolved in an acid under strictly inert conditions (e.g. in phosphoric acid), the deviation from the stoichiometry is directly attributed to the U(IV)/U(VI)-ratio in the solution. If surplus oxygen is present in the sample, as it is the case in hyperstoichiometric $(Th,U)O_{2+x}$, an equivalent amount of uranium atoms is oxidized to U^{6+} during dissolution. This reaction directs to initiate the analytical task of determining small amounts of U^{6+} in the presence of a quantity of U^{4+} and Th^{4+}. This task can be solved by electrochemical techniques, most usual by controlled-potential coulometry. In this method first the U^{6+} ions in the phosphoric acid solution are reduced at a fixed potential above a mercury cathode, at the same time the current is measured. Following quantitative oxidation of the entire uranium, present in the solution, to U^{6+} by chemical oxidant (e.g. Ce^{4+} solution), a second reduction is performed and current is measured again. The ratio of the two current values after correction for background etc. is then a measure for the oxygen-to-metal ratio in the sample.

The main advantages of this technique are

- only inexpensive devices are needed
- the techniques are relatively simple, even when radioactive samples are to be analyzed; sample preparation and calibration pose no problems
- owing to the excellent detection limit, small samples can be used to determine small deviations from exact stoichiometry
- because of subsequent determination of U^{6+} and U^{4+} in the same solution, the methods allow also to determine the absolute amount of uranium in the sample investigated.

2.3 Structural analysis

In order to demonstrate the mixed crystal structure, an X-ray photograph according to Debey-Scherrer is taken. The $(Th,U)O_2$-kernels are pulverized. The powder is melted in a capillary tube. The X-ray photograph is taken in the Debey-Scherrer chamber, thereupon it is developed. By comparing it with standard photographs, a possible existance of mixed crystals is determined. Beginning with 5 % UO_2, separate UO_2 lines can be observed.

2.4 Physical properties

2.4.1 Density and porosity

Caused by the powder-metallurgical fabrication way of pellet fuel there remains a residual porosity inside of the pellets. This porosity consisting of open and closed pores complicates the exact measurement of the bulk density. On the other hand, the pores have been understood to be a structural element of the fuel for its in-pile performance: the compensation for matrix swelling requires a controlled shrinkage of pores. Thus, in addition to the bulk density the amount of open and closed porosity must be determined.

- geometrical density -

Calculating the pellet density from the pellet weight and volume has not a sufficient accuracy because of the existence of surface damages as cracks, chips a.s.o.

- buoyancy-method -

The pellet-volume is determined by measuring its buoyancy weight in a suitable liquid. Deviations from the exact density are caused by the fact, that the liquid medium can penetrate into the open pores. This can be by-passed by using a non-wetting buoyancy medium as mercury, but no further utilization of the pellets is possible in this case.

- penetration-immersion-method -

By this method, both the bulk density and the amount of open and closed porosity can be determined. The method is based on the measurement of the pellet's dry mass, saturated mass and the suspended mass in an immersion liquid. The measurement procedure runs in the following way (compare Figs. 2.1 - 2.3):

- Drying the pellet at 150°C in vacuum
- Weighing the dry mass D (Fig. 2.1/1)
- Filling the open pores with the immersion medium by means of vacuum impregnation (Fig. 2.1/2)
- Determination of the suspended mass S (Fig. 2.1/5)
- Measurement of the saturated mass, i.e. the mass of the pellet with liquid-filled open pores (Fig. 2.1/7)
- Check of dry mass D again

Formulas for calculating the bulk density ρ_6 and the amounts of open and closed porosities, p_{op} and p_{cp}, are given in Fig. 2.2.

Various penetration immersion liquids can be used, KWU has a lot of experience using m-Xylene.

The precision of this method is high: the relative standard deviation for ρ_{UO_2} is $\pm$ 0.05 %, the standard deviation for p_{op} and p_{cp} is $\pm$ 0,03 Vol. %.

2.4.2. Thermal conductivity

The thermal conductivity of pellets can be determined by measuring the thermal diffusivity if the specific heat and the bulk density are known. The measurement of the diffusivity is performed by recording the transmission time of a heat pulse from the top end to the back end of the sample. The thermal diffusivity α is given by

$\alpha = k \cdot l^2 / t_{0.5}$ l = sample length, $t_{0.5}$ = half-life period

To generate well defined heat pulses, a laser-pulse technique is very suitable (compare Fig. 2.3).

2.4.3 Specific surface area

The measurement of the specific surface area is a less common characterization method for pellets, but can be interesting in combination with the amount of adsorbed moisture.

Well sintered pellets have specific surface areas of less than 0,1 m^2/g. In this range, the volumetric methods have no sufficient accuracy. Therefore gravimetric methods are normally used.

By gravimetric methods, the weight gain of a pellet sample by adsorption of gas molecules at low temperatures is measured directly with a microbalance. A sensitivity of 0,1 µg of the microbalance and the use of a gas with a high density in the condensed state (Kr for example) is required to determine surface areas of $\geq 100\ cm^2/g$.

In order to avoid effects coming from buoyancy, a sample of the same volume should be used as a reference sample.

2.4.4 Solid phase analysis

Phase analysis of mixed oxide fuel material is important with respect to the manufacturing technology and to the inpile behavior. The physical state of the original material-kernels or powders - influences the sintering process because the formation of solid solutions may proceed by the same transport processes in the same temperature range as the sinter densification. A non-equilibrium state of the fuel pellet can lead to a change of the fuel properties during irradiation, because of the thermal and fission included activation of diffusion processes.

Phase analyses usually is performed by determining the lattice parameters by means of x-ray analysis. Diffractometer measurements are applied as well as the Debey-Scherrer technique, both in the well known manner.

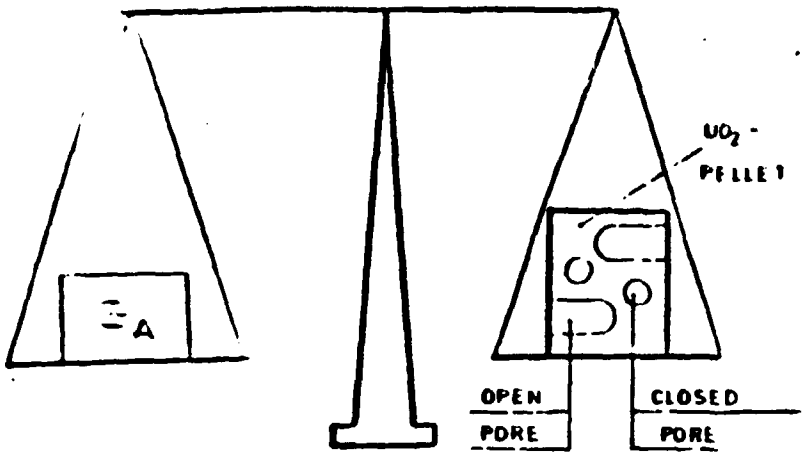

Weight in Air

G_A Weight of dry pellets in air

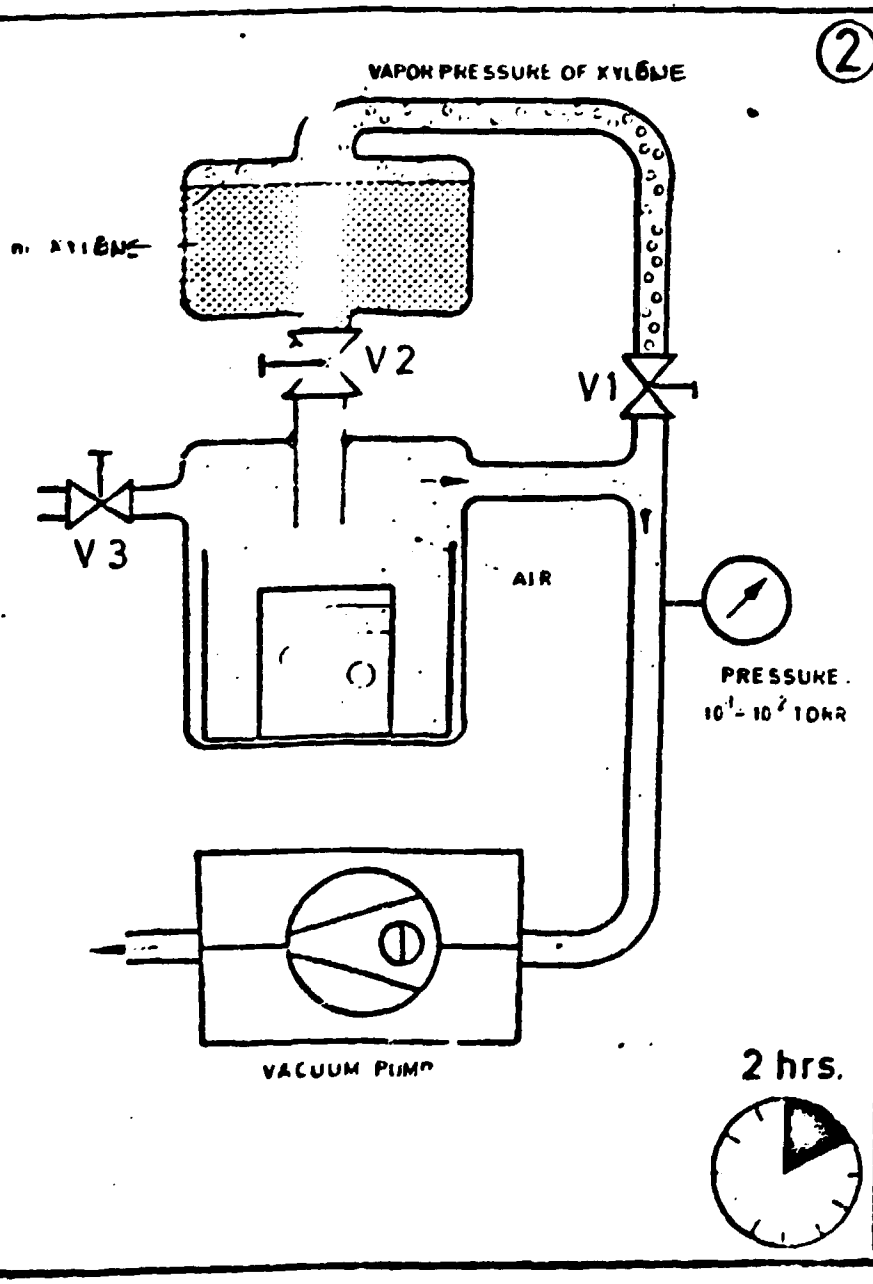

Impregnation

a) Turn on pump with valve V1 open, valves V2 and V3 closed (about 5 min.)

b) Valves V1, V2, and V3 are closed for 2 hrs at a pressure of 10^{-1} to 10^{-2} torr.

c) Valve V2 is opened filling the open pores of the pellets with m-Xylene

d) Valve V3 is opened, air enters, pump is turned off.

Fig. 2.1a: Density measurement by immersion method

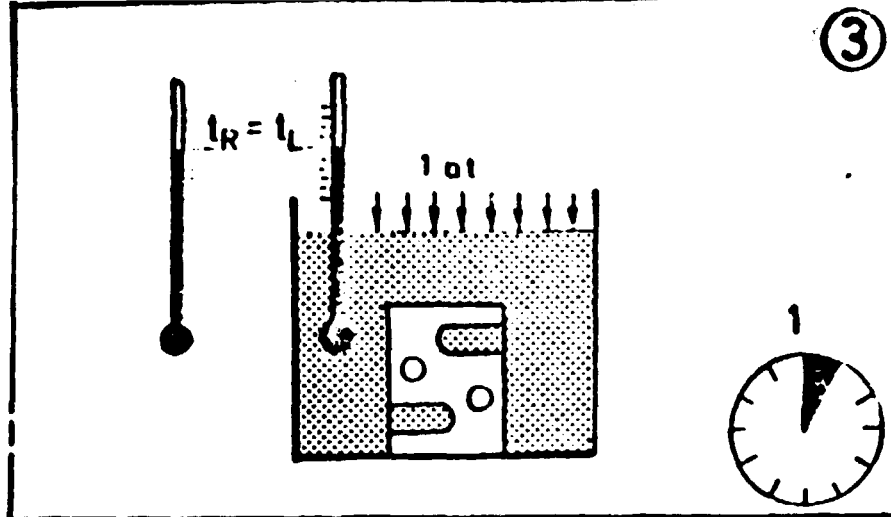

Adjustment of Weight Controlling Factors

a) Open pores are totally filled with m-Xylene

b) Temperature of liquid brought up to room temperature

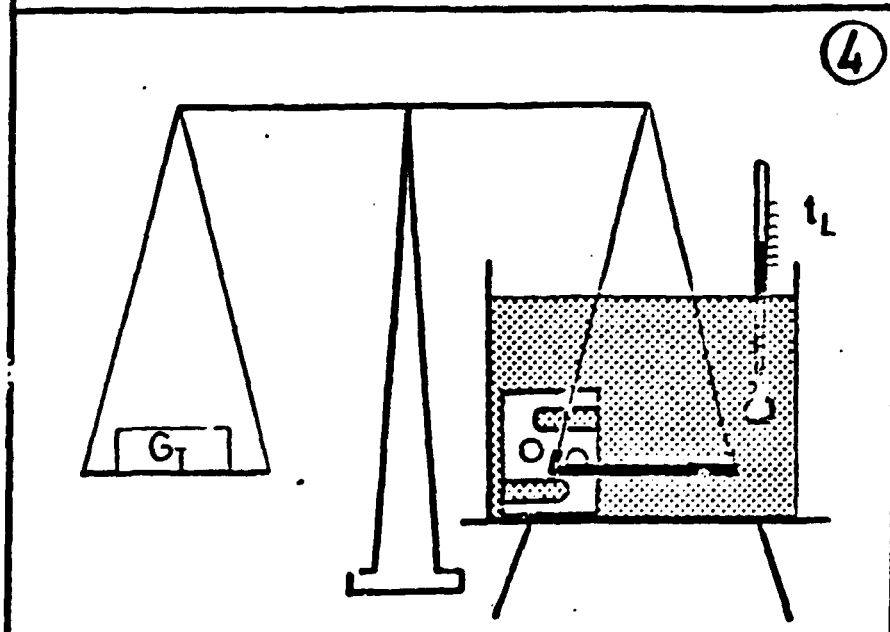

Determination of Immersion Density of Impregnated Pellet in m-Xylene

G_T Tare weight

G_P Weight of impregnated pellet in m-Xylene

The density of m-Xylene is found by measuring its temperature and locating on a graph.

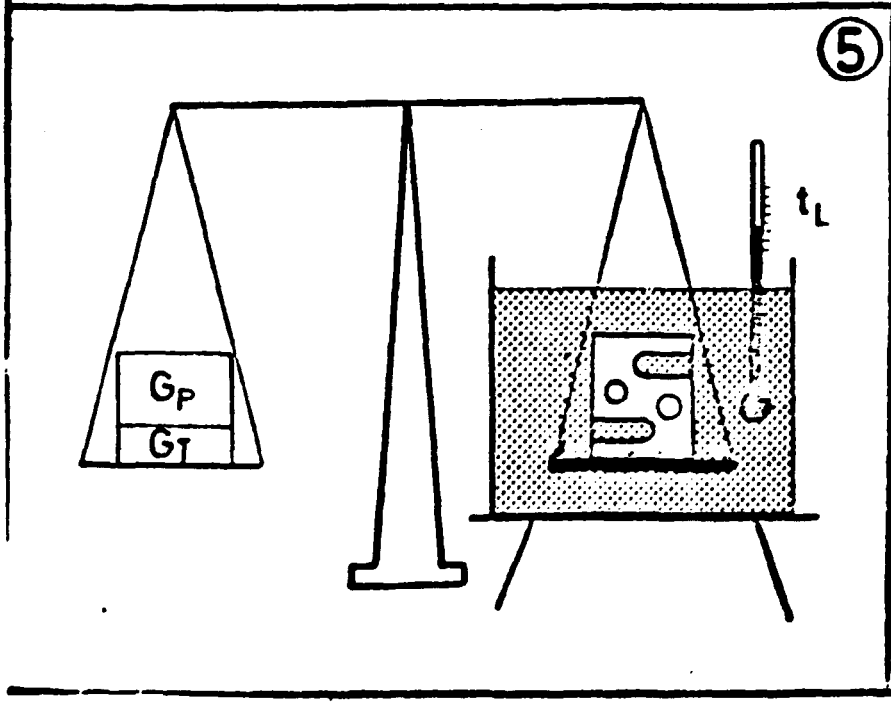

Fig. 2.1b: Density measurement by immersion method

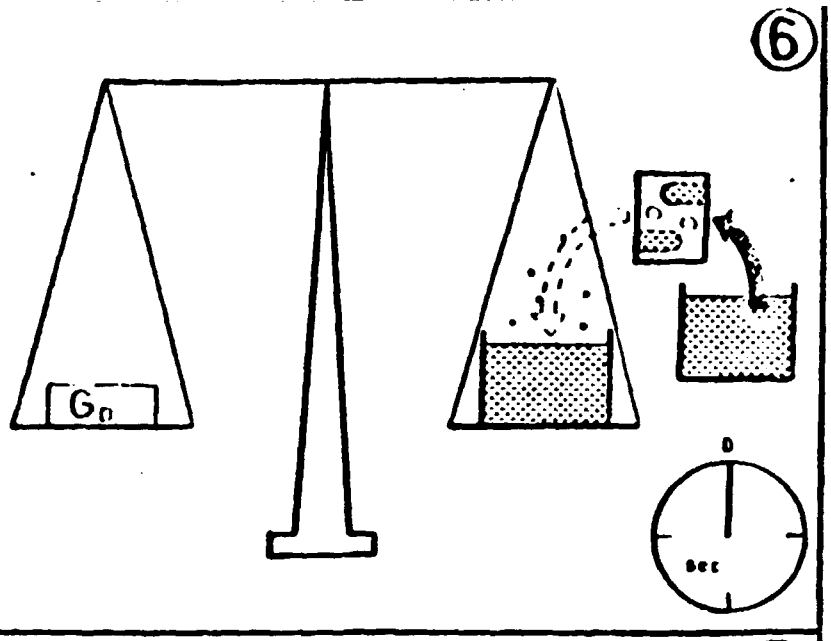

Weight Determination of m-Xylene filled Open Pores

G_D Weight of m-Xylene filled dish

G_{imp} Weight of pellet and m-Xylene impregnated pores

The measurement time is recorded to determine a correction factor for evaporation of m-Xylene

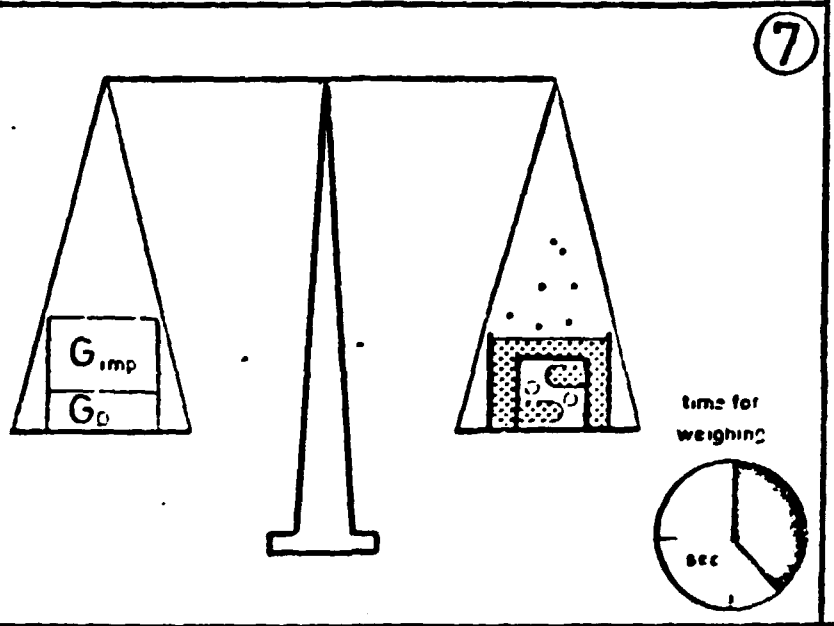

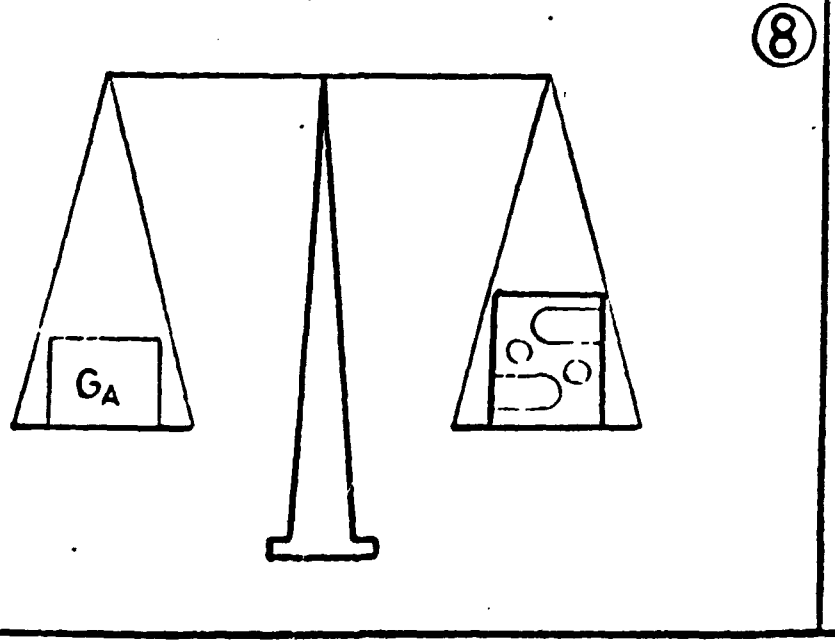

Control of Weight Measurement in Air

After drying, the pellet is weighed again.

Fig. 2.1c: Density measurement by immersion method

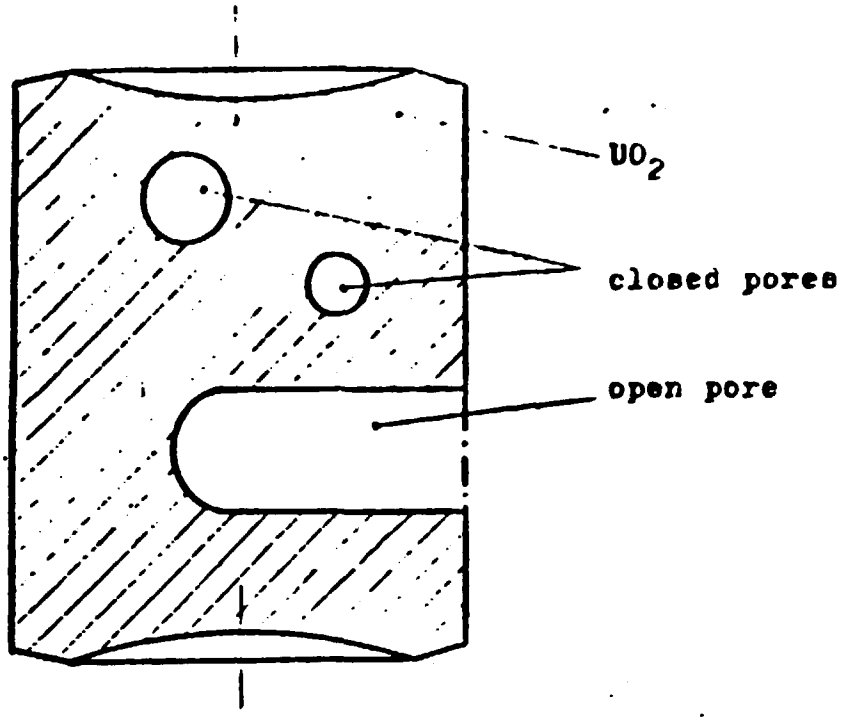

W_{dry} = dry weight

W_{sat} = saturated weight

W_{susp} = suspenden weight (pellet saturated)

V_{pell} = pellet volume

V_{cp} = volume of closed pores

V_{op} = volume of open pores

V_{UO_2} = volume of UO_2 without pores

x = density of m-xylene

pell = pellet density

TD = theoretical density of UO_2 (10,96 g/cm^3, natura)

P_{op} = open porosity (percentage of total porosity)

Fig. 2.2: Calculation of density and open porosity

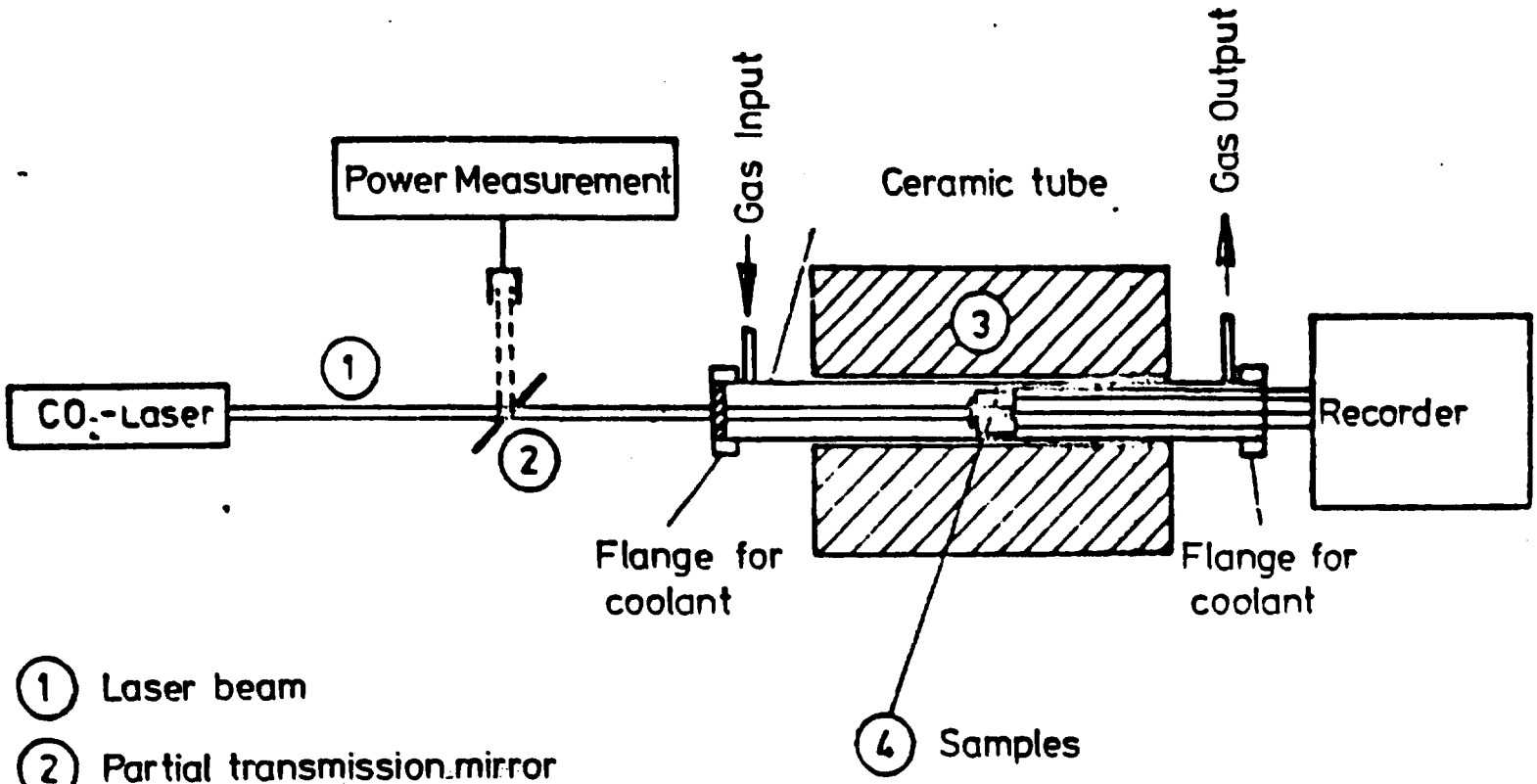

Fig. 2.3: Experimental set-up for the measurement of thermal diffusivity

3. Performance

3.1 Description of the former D_2O-Th-program

Within the former R & D-program to develop a D_2O-Th-Breeder Reactor, investigations were performed to test the irradiation behavior of fuel rods containing vibratorily compacted sol-gel derived $(Th,U)O_2$-kernels. 14 test fuel rods were fabricated, each containing two kernel size fractions

- 75 % between 630 /um and 1000 /um diameter and
- 25 % between 33 /um and 100 /um diameter.

The kernels were compacted by vibration into the cladding tube to a smeared density between 81 % and 83 % of theoretical density (th.D.). Zircaloy-4 was used as cladding material for 8 rods resulting in an outer diameter of 11.77 mm, wall thickness of 0.62 mm and 6 rods of 10.75 mm outer diameter with a wall thickness of 0.72 mm. Table 3.1 summarizes the irradiation program.

3.1.1 Investigations on sol-gel derived $(Th,U)O_2$-kernels

The irradiation tests were prepared to begin with out-of-pile studies on the kernel properties as density, microstructure, stoichiometric composition of the UO_2-part, water content and stability of kernels while being calcined. The results are presented in Table 3.2.

3.1.2 Investigations on kernel batch properties

Continuing the out-of-pile studies, restructuring processes within a kernel batch were investigated at temperatures about 2500°C, similar to those within a fuel rod under operation. The tests showed a zone refinement process, i.e. a shifting of the U/Th-ratio. In less than 2 hours, the fuel was completely redistributed by decomposition of the kernel structure. A central void developed; the colder outer periphery was enriched with uranium (Fig. 3.1). In contrast to the original U/Th-ratio (1 : 40), the figure now was determined to 1 : 15 - 18 at the edge with a depletion of uranium in the hot center.

Additionally, the stability of kernel batch and cladding was examined. It was found that a vibratorily compacted fuel column, being exposed to pressure, supports the cladding tube well, and in so far as, below a defined stress limit, it reduces its perhaps existing oval shape (Fig. 3.2).

Using a higher packing density, i.e. a second fine fraction, the supporting effect is further improved.

3.1.3 Objective of the irradiation program

The objectives of the irradiation program using the experiences from out-of-pile studies can be summarized as follows:

- Investigation of the irradiation behavior of vibro-compacted fuel up to $50 \cdot 10^3$ MWd/t
- Influence of the rating, power cycling and ramping on the performance of vibro-compacted fuel
- Investigation of fission gas release from vibro-compacted fuel
- Investigation of the relocation behavior of vibro-compacted fuel especially under the aspect of restructuring the virginal fuel columns and of equilibrium structure
- Investigation of redistribution of uranium in the mixed-oxide fuel
- Investigation of the thermal conductivity of restructured vibro-compacted fuel
- To check if there is any evidence for fuel rod failure mechanisms being typical for vibro-compacted fuel
- To provide spent fuel to investigate the dissolving characteristic and the refabricability of Zircaloy-clad vibro-compacted Th/U-mixed-oxide fuel

Originally, the single rod irradiation was planned to be prerunning a bundle experiment with a full size prototype fuel element of a D_2O-Th-reactor. By this fact the first 3 experiments were planned to be long running to provide the data basis for the design and the licensing of the bundle irradiation. The following experiments should mainly answer questions of the behavior of vibratorily compacted fuel under transient conditions. The last part of the program was planned to be a prerunning test series to the bundle experiment.

3.2 Experimental techniques

The in-pile testing was performed in the test reactor FRJ2 of the KFA-Jülich. Within the FRJ2-reactor, boiling water loops serve for testing the irradiation behavior of fuel rods under operation conditions. The used irradiation positions were 2V6, 2V7 and 2V8, and the irradiation rigs were connected to the boiling water loops LV9c and LV9d. The rig contained in an outer tube a

pressure vessel which was centered by the flow divider. Each of the seven irradiated rigs (Fig. 3.3) contained two test fuel rods being arranged one upon another. The test rods of 278 mm length were sealed at their ends by an Al_2O_3-respectively natural UO_2-pellet without a fission gas plenum. Three rods were instrumentated with a pressure transducer to measure the rod internal gas pressure during the irradiation. The rods were surrounded by guiding discs which limited the size of the steam bubbles, suppress convection currents, therefore providing very uniform heat transport conditions (Fig. 3.4). The externally flowing coolingwater cooled the primary water through the pressure vessel. The fuel rod power was continuously measured during irradiation, by determining the heat output of the cooling-water. From this value, the heating, which comprises gamma-absorption and moderation of neutrons within the rig outside of the fuel rods, was subtracted. This heating had been determined in a pre-test for each of the applied irradiation positions and included all influencing parameters up to 1972. Since 1973, the experiments were cooled by a separate cooling cycle. This resulted in additional calculations for correcting the heat flow from the warmer moderator into the rig. The accuracy of the total power measurements was about 3 %. The irradiation and burn-up data were recalculated by the computer program BRUT1. The release of fission gas was determined by the, in the shut-down periods measured, inner pressure. In Fig. 3.5, the pressure, calculated to room temperature, is plotted against the average burn-up of a fuel rod. In addition, the average linear heat power and the release rate (as relation of released to generated fission gas) are marked. The surface temperature of the fuel rods depends within the region of bubble boiling on the water pressure; insignificantly on the heat transferred per unit surface which was between 98 and 173 W/cm^2. The surface temperature at a water pressure of 118 bar (128 bar) was 601 K (606 K).

3.3 Irradiation history

According to the objectives of the irradiation program, 14 test fuel rods were irradiated in 7 irradiation rigs between 4 h and 673 full power days (Table 3.1). The maximum burn-up was about 45.000 MWd/t (Th+U) at a linear heat rating of about 700 W/cm. The rods were exposed to many load cycles. Those rods being long-term irradiated were changed in their positions several times to balance the burn-up dependent power decrease. By this and in changing the charge in the adjacent irradiation channels strong power increase (power ramping) occured. The data for the inner pressure of fuel

rod e.g. RBE25 are plotted against the irradiation time in Fig. 3.6. Additional irradiation data, e.g. fission rate of U-235 $S_{max.}$ (FIFA), temporal and local highest thermal load $B_{max.}$, irradiation time, begin and end of irradiation, number of power cycling, are given in Table 3.1.

3.4 Post-irradiation examination results

The out-of-pile investigations gave a first reference for the irradiation behavior of vibratorily compacted $(Th,U)O_2$-fuel rods. Therefore, in continuing with in-pile testing and post-irradiation examinations, the following aspects with regard to fuel behavior and operation had to be considered:

- structure of irradiated fuel
- uranium distribution within the fuel rod
- fission gas release
- cycling behavior of the fuel
- failure effects

3.4.1 Structure of irradiated fuel

According to the high central temperature at linear heat ratings beyond 400 W/cm, the original structure of the fuel changed into a typical structure after being irradiated. Fig. 3.7 shows composite radial micrographs of a fuel rod after 25,2 days irradiation. Five structural areas could be determined

- non-sintered kernels in a loose packing
- luted kernels
- well sintered and densified structure
- dense sintered structure with lenticular fission gas bubbles
- central void formation

In Fig. 3.8, those points of the same type of microstructure are plotted into the longitudinal cross section of the fuel volume. The lines of the same phase can be interpreted as isothermes. The development of the different phases is dependent on the thermal load of the fuel rods. The gamma-scans in Fig. 3.9, corresponding to the isothermes, show relative power distributions in axial direction. The burn-up distribution was according to the flux profile in the irradiation channel.

3.4.2 Uranium-distribution within the fuel rod

The U-distribution in $(Th,U)O_2$-fuel rods after 25,2 days irradiation is demonstrated in Fig. 3.10. The data were measured at two positions with the highest heat ratings of about 405 and 575 W/cm. As previously shown in out-of-pile tests, the uranium relocated towards decreasing temperature. The effect was more significant at higher fuel rod thermal loads (steeper temperature gradients) than at lower gradients. α-Autoradiographics of the longitudinal and cross sections of the long-term irradiated fuel rods demonstrated an increased α-activity in the center of the sintering zone (Table 3.3). U-233 and U-234 being the main emitters with high α-activity were found to less than 1,5 %; they were concentrated at the outer periphery. This U-redistribution would be favourable for the irradiation behavior of fuel rods. As the heat was produced at the periphery, the heat passage was short, therefore providing low fuel temperatures. This is in contrast to U/Pu-fuel rods, where by the bred Pu, the heat will be produced within the fuel rod center.

3.4.3 Fission gas release

Table 3.4 lists the measured values for

- the gas contained in the rod
- the available volume of the fuel rod
- the fission gas release factor η
- the gas pressure in the fuel rod
- the change of the available fuel volume related to the total volume (directing to swelling).

At the end of irradiation, fuel rod RBE38 leaked and fission gas poured into the water; the irradiation stopped. The leak, however, sealed again at room temperature, so that the fuel rod's internal pressure remained with greater than 50 bar. By post-irradiation examination, the leak could not be determined; gas-analysis confirmed that the pressure had been produced by stabile fission gas and Kr-85. The rods being irradiated for 25,2 days showed a fission gas release of rather twice the time (58 - 61 %) than released by the rods with 37,9 d (25 %) and 113,3 d irradiation (32 %). This strong deviation had been probably related to determination failures. Normally, a total fission gas release of about 30 - 40 % (for this kind of fuel and existing heat ratings) would have been dissolved during operation.

An irradiation test performed (113 d) gave much information by measuring the gas pressure in a fuel rod. The initial peak had been reduced within short time; then the internal pressure increased rather linear, by this directing to a homogeneous release rate. Power cyclings generated additional fission gas. This could be recognized especially in a specified program with 11 power cycles (Fig. 3.6).

3.4.4 Cycling behavior of the fuel

The sagging of fuel by enlargement of the fuel rod cladding under temperature and power cycling was investigated. Power cycling of the fuel can result in two effects:

- the original fuel can plastically extend the cladding and then sag during cooling
- fuel, being redistributed, with a central void formation can break, so that fuel fragments tumble down within the central channel, and lead in the lower part to a power increase.

During irradiation, special cycling programs were performed to demonstrate, that vibratorily compacted fuel columns did not extend the cladding. None of the investigated fuel rods being operated under a great number of the normal reactor shut-downs showed significant diametral changes of the cladding tube by fuel swelling, much less effects of fuel tumbling. In general the increase in diameter was less than $6 \cdot 10^{-3}$ (Table 3.4). The increase of fuel rod length essentially, was in the region of the normal irradiation induced growth of Zircaloy, although no plenum had been employed and some rods were operated under a big number of power cyclings.

3.4.5 Defects

A number of defects occured during irradiation. They were generally contributed to deposits on the heating surfaces. After having installed additional activated charcoal filters into the pressurized water cycle, to avoid water impurities, the development of deposits disappeared, especially in the long-term irradiation tests. By local heat blocks, the deposits effected temperature elevations in the cladding tube, which resulted in local oxidation and cladding failure (RBE27, 29, 35, Fig. 3.11). As the fuel, directly beyond the defect, remained unchanged, a causal contribution of the fuel rods were instrumentated with a pressure transducer, therefore the leakage could be controlled by measuring. In these cases, the leak at first led to a more or less fast increase of the fuel rod inner pressure giving

no activity signals. In one case, in spite of a defect, the test could be continued for 4 h until the activity released a shut-down of the reactor. No interactions between penetrating water and fuel could be determined in the post-irradiation examination of the failed fuel rods. Only directly closed to the leak, an oxide layer, decreasing with increasing distance was found. In none of the cases fuel kernels reached the circuit.

3.5 Reprocessing

For reprocessing studies, sections of a "D_2O-Th-Breeder-Reactor"-fuel rod (RBE-30) were supplied to Hoechst. The fuel rod contained vibratorily compacted $(Th,U)O_2$-kernels in a Zircaloy-cladding, achieved a burn-up of 2660 MWd/t and was cooled up to dissolution tests 96 days and for extraction 158 days. The reprocessing used the acid THOREX-process with an acid deficient feed solution.

The fuel rod was cut at KFA into about 10 mm long sections. Fuel ranging in size from approximately 0.5 mm to 5 mm could be poured from the cut fuel sections. The size of kernels before irradiation had been smaller than 0.8 mm. Therefore, the irradiation apparently produced only localized sintering of the fuel near the axis of the rod. Experience has shown that most fuels cannot be freely poured from the sheared cladding sections but must be dissolved out by THOREX-reagent. Therefore, the Zircaloy cladding was placed into the dissolver solution together with the fuel in order to investigate the amount of Zircaloy being dissolved. The reprocessing tests showed that the dissolution time of fuel took 40 - 50 hours during which 17 % of the Zircaloy were also dissolved. The feed adjustment and extraction were performed without incident.

3.6 Evaluation

The out-of-pile investigation clearly demonstrated that suitable fuel rods can be manufactured using spherical sol-gel derived $(Th,U)O_2$-particles and vibro-compaction. The sol-gel process provides kernels of high density. A binary mixture of two diameter fractions can be filled into the fuel rods with a smeared density of 82 % theoretical density using the infiltration method. Chemical and structural analysis show a very low level of impurities in the fuel and a homogeneous mixed-oxide distribution. Vibratorily compacted fuel columns show a very good geometrical stability within the cladding especially under thermal cycling and outside overpressure.

An irradiation program was performed using test rods having burn-ups up to 50.000 MWd/t. During the irradiation of the seven experiments (each with two test rods) heat ratings up to 680 W/cm, power ramps between 520 and 650 W/cm and special cycling programs could be realized without typical fuel rod failures. Failures occuring could be attributed to formation of deposits due to impurities in the capsule.

During post-irradiation examination, none of the fuel rods showed significant diameter changes or fuel swelling. The gamma-scan values agreed with those calculated for the power distribution prior to the experiments. The fission gas release rate was in between 28 and 61 %. The characteristic fuel structures i.e. the non-relocated outer fuel region, the sintered kernel region, the fully restructured inner fuel zone and possible formation of central voids will appear within a few days of irradiation. Afterwards the changes in the fuel columns are very small. Relocation of the fissile uranium towards the cooler outer fuel zone was verified during the post irradiation tests.

Irradiated fuel from the experiments was also successfully reprocessed in an experimental device in the hot cell facility using the THOREX-process. The irradiated fuel material could be dissolved without any problems. The investigations on the performance of Th-fuel technology within the D_2O-Th-Breeder study had already reached a certain status; but only in so far as it is concerned Th-fuels as vibratorily compacted $(Th,U)O_2$-kernel fractions. To get knowledge about the irradiation behavior of pelletized $(Th,U)O_2$-fuel, further irradiation tests must have to be performed.

Characteristics													Irradiation											
irradiation rig	fuel element test rod RRE-	with pressure transducer = +	fuel			isolating pellet			cladding tube				water pressure	surface temperature	max. heat rating	thermal load at leakage	heavy metal burn-up (Th+U)	fission rate U-235 (fifa)	axial burn-up ratio	irradiation time	number of load cycles	begin/end of irradiation	irradiation report	
			design	total mass	density	material	diameter	height	material	autoclaved = +	wall thickness	outer diameter												
				m_{oxid}	ρ/ρ_{th}								P	T	Λ_{max}		S_{max}	$\bar{\Lambda}/\Lambda_{max}$						
				g	%		mm	mm			mm	mm	bar	K	W/cm		MWd/t	%	1	d		date	number date	
LV9.2	25	-	(Th,U)O_2-kernels with 4.45% uranium 75% with ∅30 µm to 1000 µm diameter 25% with 33 µm to 100 µm diameter	199.7	81.7	xxx	xxx	xxx	xxx	-	xxx	xxx	128	606	595	xx	2462	6.16	0.815	25.2	6	28.02.1968	IRB73-1-Re	
-E13	26	-		198.4	81.2										635	xx	2627	6.57	0.976			28.03.1968	9.12.68	
LV9.3	27	+		198.7	81.8	UO_2 nat.	10.37	5.5	Zircaloy-4		0.62	11.77			597	410	9090	22.5	0.803	113.3	49	06.09.1968	IRW1308-Re	
-E16	28	-		199.8	82.2										646	xx	9764	24.2	0.965			17.03.1969	11.07.69	
LV9.3	29	+		199.7	81.8										633	415	3075	8.68	0.789	37.9	8	18.03.1969	IRW1308-Re	
-E29	30	-		198.9	82.2										685	xx	3312	9.35	0.968			21.06.1969	04.12.69	
LV9.3	35	+		196.4	81.5					+			118	601	559	ML	44664	134.4	0.897	673.2	94	08.07.1971	ZRBIB16/75	
-E31	36	-		196.7	82.0					+					668	xx	45195	136.0	0.956			08.03.1975	10/75	
LV9.2	31	-		155.1	82.6		9.3			-					644	xx	8616	21.6	0.823	78.6	25	08.11.1968	IRB1308-Re	
-E17	32	-		152.9	81.9	Al_2O_3	9.3			-					668	668	8901	22.3	0.968			08.04.1969	30.05.69	
LV9.2	34	-		153.9	82.0		9.2	7		-	0.72	10.75			613	xx	28	0.06	0.807	0.2	1	08.11.1969	IRW1308-Re	
-E30	33	-		154.2	82.1		9.2			-					634	xx	29	0.06	0.965			09.11.1969	05.12.69	
LV9.2	37	-		154.8	82.9		9.3			+					583	xx	49591	149.4	0.899	603.7	87	08.07.1971	ZRBIB16/75	
-E32	38	-		151.5	81.1		9.3			+					595	CL	50265	151.5	0.957			09.12.1974	12/75	

ML= Membrane leak
CL= Cladding leak
RRE-27,-29 and -32 leaked by deposits and local oxidation

Table 3.1: Data of the irradiation program

density (%th.D)	UO_2:ThO_2 ratio	UO_2 stoichiometric composition	water content (ppm)	microstructure	stability while being calcined
98-99	1:40 90% U-235	2.030 ± 0.012 homogeously distributed	< 20	two zones -fine crystalline kernel -coarse crystalline surface layer	< 2000°C, kernels unchanged, > 2000°C, kernels started luting

Table 3.2: $(Th,U)O_2$-kernel properties

nuclide	atom part	half-life period	activity part
	%	y	%
Th 232	97.0	$1.405 \cdot 10^{10}$	0.07
U 233	1.4	$1.59 \cdot 10^{5}$	83.1
U 234	0.4	$2.44 \cdot 10^{5}$	15.5
U 235	0.1	$7.04 \cdot 10^{8}$	0.001
U 236	0.6	$2.342 \cdot 10^{7}$	0.2
U 238	0.5	$4.47 \cdot 10^{9}$	0.001
Pu 240	0.001	6537	1.4

Table 3.3: Parts of α-activity of the α-emitters

irradiation rig	test fuel rod RBE -	cladding defect = +	average heavy metal element burn-up	average change of length 1/1 cold	average diametral changes / cold	gas (1,0132 bar, 293 K)	release rate	rod's final pressure (293 K)	available volume		
									before Va	after Vb	$\frac{Va - Vb}{V_{fuel\ rod}}$
			MWd/t	$.10^4$	$.10^3$	ml	%	bar	cm^3		%
LV9.2	25	-	2007	xxx	2,36	19,03	61,4	2,08	3,50	xxx	xxx
-E13	26	-	2564	xxx	1,87	11,54	58,4	2,40	3,81	xxx	xxx
LV9.3	27	+	7299	-1,90	4,25	xxx	31,2	xxx	3,80	xxx	xxx
-E16	28	-	9422	-1,61	4,84	15,99	24,0	7,34	3,72	3,31	2,00
LV9.3	29	+	2426	-4,75	5,86	xxx	28,3	xxx	3,85	xxx	xxx
-E29	30	-	3206	-3,54	-0,59	6,16	26,0	2,67	3,84	3,47	1,82
LV9.3	35	+	40064	11,49	1,27	47,07	46,3	12,62	4,06	3,78	1,39
-E31	36	-	43210	8,91	5,27	143,65	47,8	49,51	3,75	2,94	4,02
LV9.2	31	-	7091	1,29	4,84	16,03	45,0	7,45	2,78	2,49	1,83
-E17	32	+	8616	0,64	5,86	xxx	xxx	xxx	2,98	xxx	xxx
LV9.2	34	-	23	2,69	0,56	too less	xxx	0,98	2,89	3,20	-1,97
-E30	33	-	28	2,59	0,93	too less	xxx	1,10	2,89	3,16	-1,71
LV9.2	37	-	44622	5,21	3,63	124,69	55,0	72,61	2,75	1,74	6,37
-E32	38	+	48164	7,46	5,02	110,50	45,0	52,08	3,08	2,15	5,99

§ with deposit

Table 3.4: Post-irradiation examination results

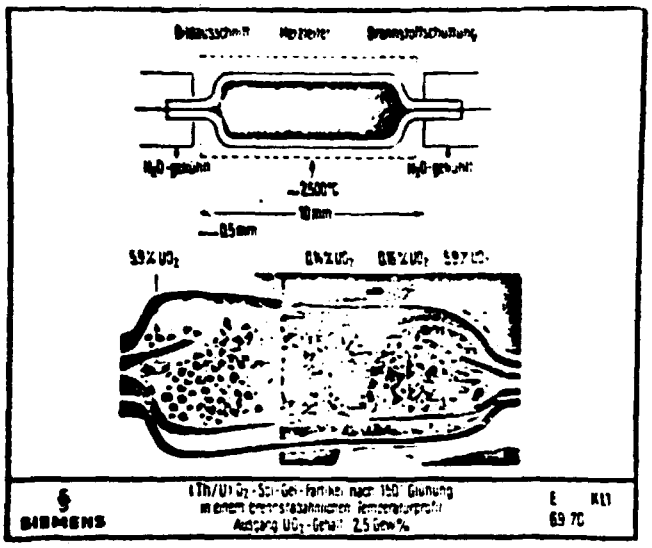

Fig. 3.1: (Th,U)O_2-kernels being calcined for 150 in a fuel rod similar temperature profile (initial UO_2-content: 2,5 %) (Siemens EZEF/KL1 6970)

Fig. 3.2: Oval-shape of fuel rods after 176 h at 140 atü /340°C and 24 h at 200 atü /340°C (Siemens EZEF/KL1 6973b)

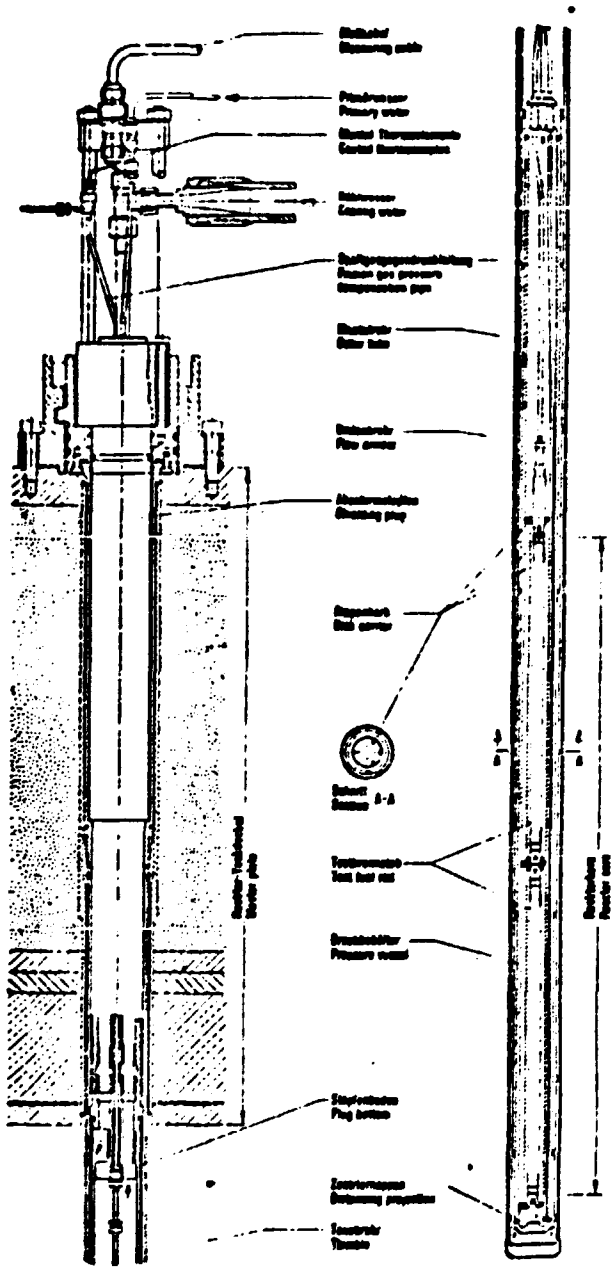

Fig. 3.3: Irradiation rig

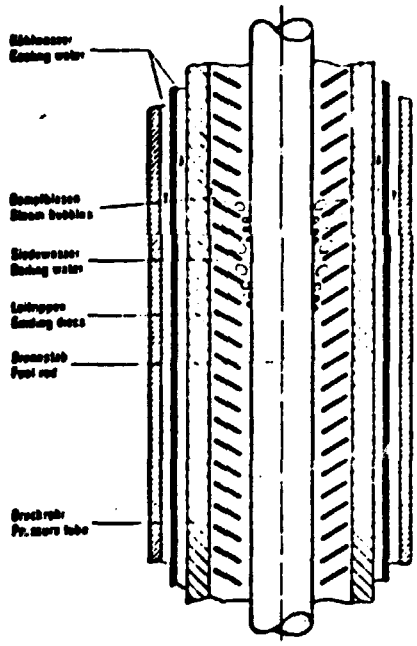

Fig. 3.4: Fuel rod cooling by boiling pressurized water with steam bubbles stabiliser.

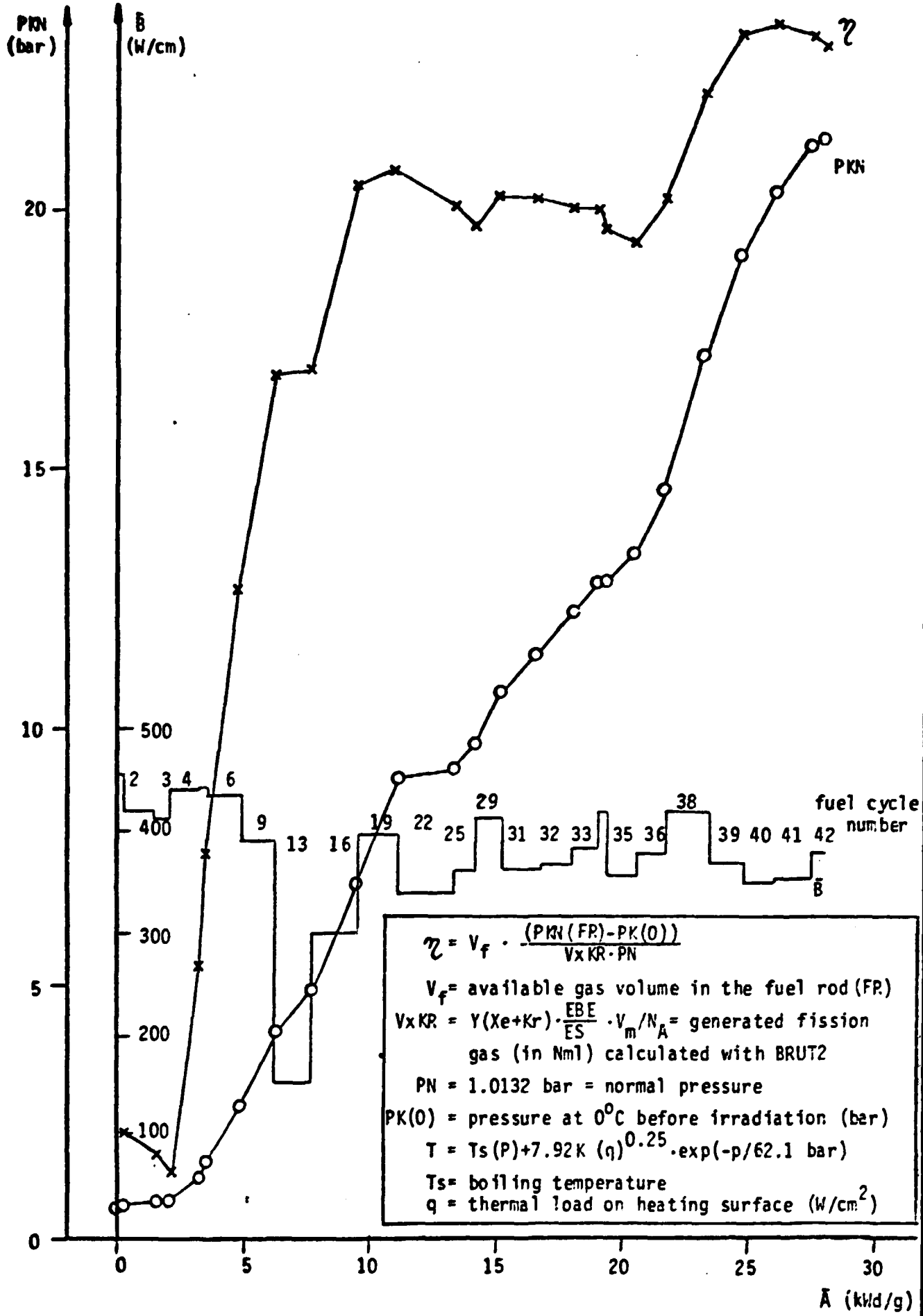

Fig. 3.5: Pressure (PKN), average linear heat power ($\bar{B}$), release rate ( ) against average burn-up ($\bar{A}$) of fuel rod RBE-35

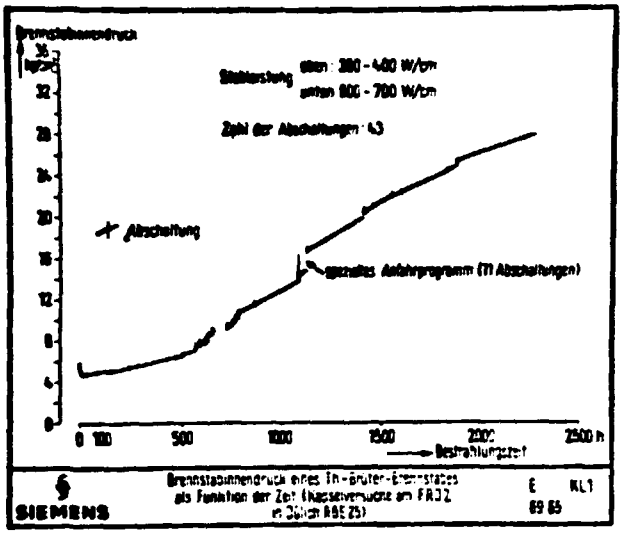

Fig. 3.6: Gas pressure in a fuel rod, measured during operation (Siemens EZEF/KL1 6965)

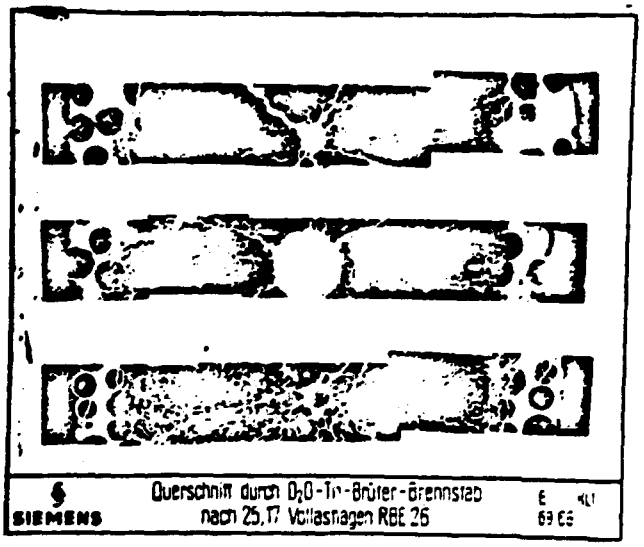

Fig. 3.7: Cross section through fuel rod RBE-26 after 25,2 days irradiation (EZEF/KL2 6968)

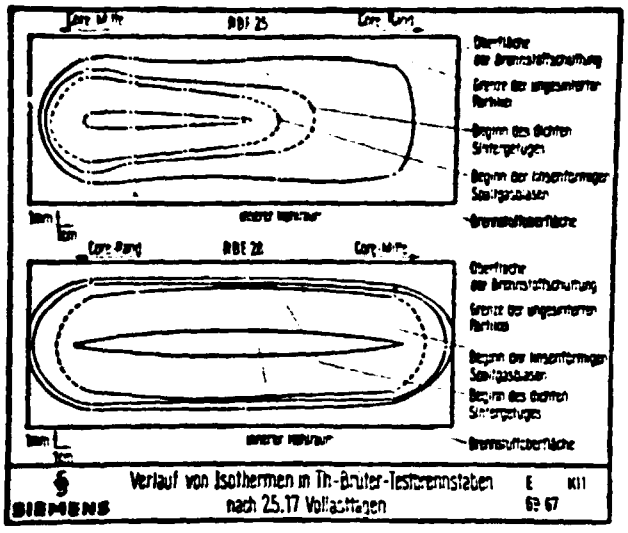

Fig. 3.8: Isotherms in fuel rods RBE-25 and -26 after 25,2 days irradiation (Siemens EZEF/KL1 6967)

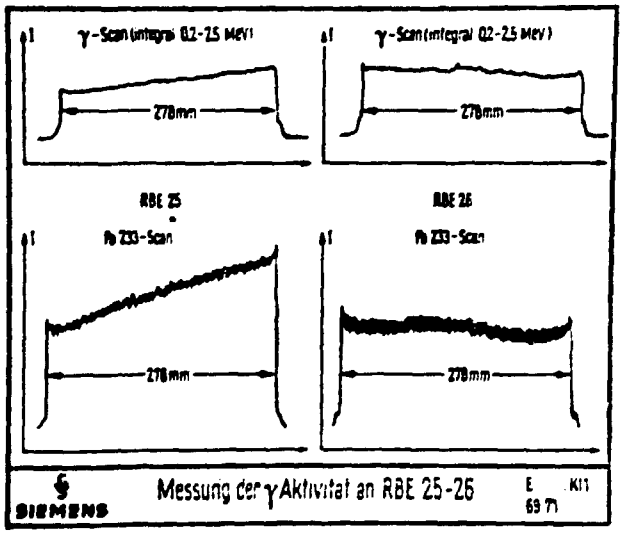

Fig. 3.9: Measurement of -activity (RBE-25, and -26) (Siemens EZEF/KL1 6971)

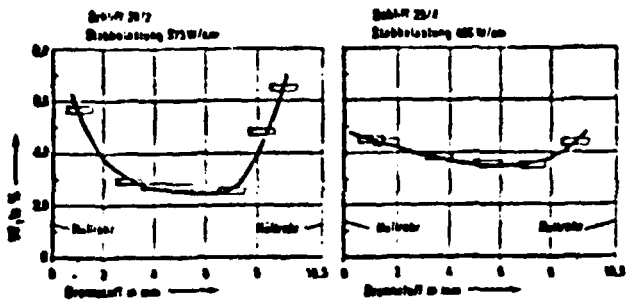

Fig. 3.10: Uranium-distribution in $(Th,U)O_2$-fuel rods after 25,2 days irradiation

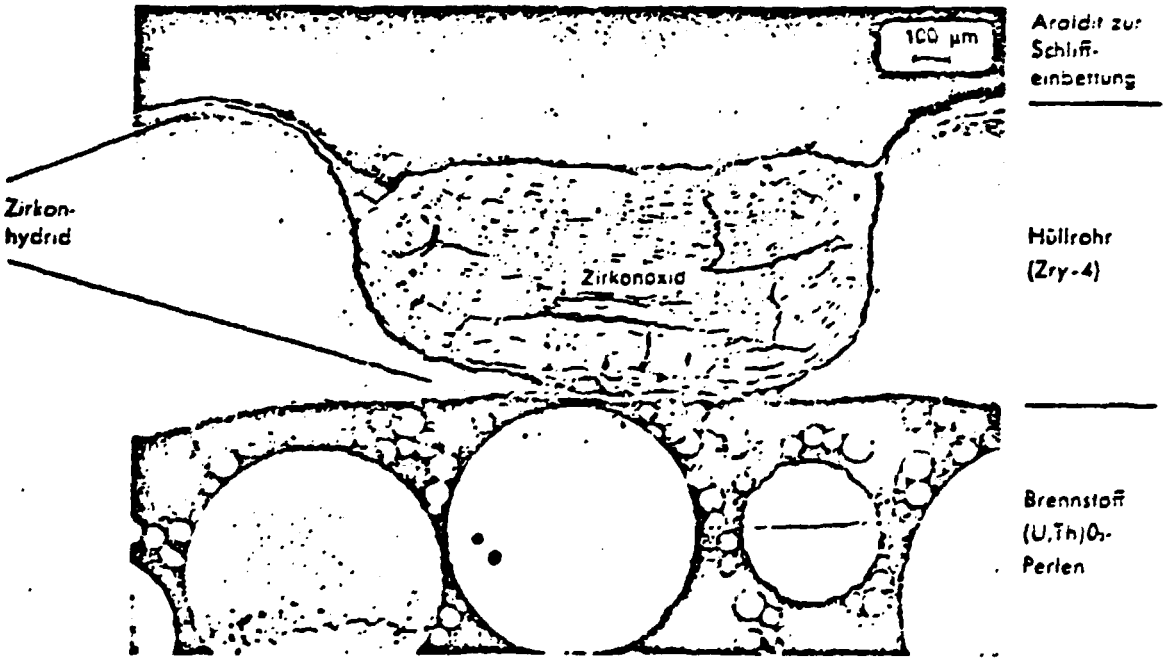

Fig. 3.11: Cross section through fuel rod RBE-32 (Zry 4-cladding, $(Th,U)O_2$-kernels, 668 W/cm thermal load, 8901 MWd/t burn-up); cladding failure occured by deposits, heat block and oxidation.

4. Literature review on performance

The general objective of this literature study has been to demonstrate the status of irradiation experience with $(Th,U)O_2$ containing fuel elements for water reactors beyond with that reported for Germany and Brazil in the other chapters. As basis the study uses subjects from the literature of Nuclear Science Abstracts (1949 - 1976), INIS Atomindex, IKK and Energy Research Abstracts for the period 1976 - 1979. As far as information on fabrication processes and development could be obtained by the available literature (Appendix), it is listed likewise. The informations are structured by the following items:

- fabrication processes (pelletizing-, vi-pac-, sphere-pac- and extrusion processes, properties)
- irradiation testing.

4.1 Fabrication processes

The various fuel element fabrication methods can use the fuel as powder, claylike material, angular particles and microspheres, prepared by either arc-fusing, standard pellet powder fabrication techniques or sol-gel processes, filled into the tubes by different routes. In general, the techniques for preparing particle fuel are described as dry and wet chemical processes. Dry processes are arc-fusing, agglomeration of powders and pellet crushing. Their products vary in size and density. Additionally, dry processes are linked with a separate conversion step and the associated handling of powders. Wet chemical methods are summarized as sol-gel or precipitation processes. The final steps of the versatile sol-gel processing can be adjusted to yield an oxide product in form of either microspheres, shards, clay or sinterable powder. The development and technologies are reported by extensively published literature /e.g. 1 - 4/. The problems of scrap recovery, -recycling, in general the question of waste treatment were not discussed.

4.1.1 Pelletizing process

Formerly, pelletized fuel had been mainly fabricated by standard powder preparation techniques (e.g. mechanical mixing, coprecipitation), granulation, pressing and sintering, mechanical sizing, finally leading to a controlled pellet. The development and manufacture by standard methods was first reported by the work of Argonne National Laboratory in fabricating ThO_2-UO_2 ceramic fuel pellets for BORAX IV reactor (1955 - 1957) /5/.

Shortly afterwards, Th/U-oxide pellets were designed for irradiation in the Indian Point Reactor (Core A 1959 - 1960) and Elk River Reactor (Core No. 1 1959 - 1960, Core No. 2 1965 - 1966) /4,6/. As part of the Light-Water Breeder-Reactor (LWBR)-program, also Th/U-oxide pellets were fabricated /7-11/. General studies on material properties, methods used for pellet fabrication, preparation for irradiation are described /5,12-19/. Recent research and development work considered also using sol-gel derived materials (sinterable powders) for pellet preparation because of the relatively low sintering temperature needed to attain moderate densities, their good homogeneity and simplicity in recycling. The gel powders are calcined, sintered and pressed into pellets. The technology for fabricating pellets, the effects on green density, of powder calcination temperature, sintering atmosphere, powder moisture content, forming pressure, preparation for irradiation are discussed /20-29/.

4.1.2 Vi-pac process

Work on the vi-pac technology, i.e. vibratory high energy compacts the dense angular $(Th,U)O_2$-fuel particles (shards) into the tube, was reported in the literature on a wide range /30-40/. The performed vi-pac studies evaluated parameters such as vibration energy characteristics, effects on fuel density, compaction time and compressive load, of particle-size distribution, preparation and suitability for irradiation.

4.1.3 Sphere-pac process

The sphere-pac process uses low energy for compaction of sol-gel microspheres by matched size fractions. Only using the infiltration of material yields in high density and most uniform packing. Contrary to vi-pac, the process will not require a complicated remote equipment for the mechanical treatment of fuel fragments into a suitable size distribution. Loading studies, investigations on attainable packing densities, equipment requirements and improvement, the use of different size fraction systems, fabrication studies and preparation for irradiation are reported /41-45/.

4.1.4 Extrusion process

Extrusion fabrication procedure can also use the sol-gel derived fuels. A pellet is produced with uniformly distributed porosity, good mechanical strength at low densities. The extrusion development work was mainly directed to the Progetto Ciclo Uranio-Torio (PCUT)-project in Italy /4,46/.

Work on characterization of powders, preparation of concentrated sols or clay by the sol-gel process, improvement of green and sintered densities was summarized /47-51/.

Most of the development effort on fabrication processes was spent on the vi-pac technology as this method generally can use the fuel material as angular particles or shards. While introducing the sphere-pac process, which indicated to be the best method for fabricating high-dense and uniform fuel, easy to handle in the recycling, the development stopped prematurely due to other program activities.

4.1.5 Properties

Furtheron, general basic information, which will be required to evaluate the fuel technology and fabrication processes with regard to interpretation of results of irradiation test performance, was obtained by studies and investigations on

- characteristics and properties of material and relation to irradiation test performance /9,10,52-59/.
- sintering behavior and grain growth kinetics /16,60-68/
- simulation of thermal gradients /69/
- water logging susceptibility /70/
- gas evolution /37,54,71/
- inhomogeneity of fuel, redistribution /72,73/
- thermal conductivity /54,74-84/
- rates and kinetics of fission gas release /39,40,54,78,84-104/

No systematic investigations on the behavior of fission products were performed.

4.2 Irradiation testing

4.2.1 $(Th,U)O_2$-fuel performance in test reactors

A number of irradiation tests was performed in water-moderated reactors to evaluate the in-pile behavior of various $(Th,U)O_2$ containing fuel rods fabricated by either pelletizing, vi-pac or sphere-pac. The irradiation program is summarized in Table 4.1.

Fuel performance was extensively studied within the Oak Ridge National Laboratory irradiation program which started in 1961. The first initial results on the performance characteristics were found to be favourable /40,53,54,68,72-80,90,91,105-119/:

- all thoria based fuels in general perform well or even superior compared to urania based fuels
- sol-gel derived $(Th,U)O_2$-fuel meets the basic performance requirements of a nuclear fuel and compares favorably with arc-fused material (Table 4.1, MTR I and NRX II)
- vibratorily compacted $(Th,U)O_2$-fuel rods perform as well as those containing pressed-and-sintered pellets at moderate heat ratings up to 300 W/cm and burnup levels about 40.000 MWd/t (Th+U)

The work continued in investigating the performance of $(Th,U)O_2$-fuel under different test conditions as

- high burnups and moderate heat ratings
- high burnups and intermediate heat ratings
- moderate burnups and high heat ratings
- processing variables effecting the irradiation performance.

Performance at high burnups and moderate heat ratings

The effects of extended burnup on microstructural changes, swelling and fission gas release rates were tested (Table 4.1 MTR I) /21,53,54,91,105, 106,108-112/. The tests demonstrated that $(Th,U)O_2$-fuel performed satisfactorily at high burnups in excess of 100.000 MWd/t (Th+U), at moderate linear heat ratings between 300 and 460 W/cm, releasing fission gas rates generally less than 20 %, showing no evidence of breakaway swelling or sudden increase in fission gas release, and good dimensional stability. In comparing pellets and vi-pac fuel, the post-irradiation examination indicated no difference in the macroscopic appearance after the extended irradiation. The available data on the structural behavior demonstrated the fuel behavior in general to be good, but not any investigation had been performed to give a statement about the relation between structure and stability.

Performance at high burnups and intermediate heat ratings

Tests were performed to study the effect of intermediate heat ratings at high burnups within the MTR II group (Table 4.1) at linear heat ratings of about 600 W/cm reaching peak burnups of about 125.000 MWd/t (Th+U)/109,110, 112/. Comparison of the rods showed that higher heat ratings led to greater grain growth and central void formation.

Performance at moderate burnups and high heat ratings

By investigating the effects of higher heat ratings (Table 4.1, ORR-loop and poolside, ETR I) /40,53,54,80,91,103,107,110,111/, it was reported that heat ratings in excess of 1000 W/cm at burnups about 22.000 MWd/t (Th+U) could be accomodated by sol-gel derived vi-pac $(Th,U)O_2$-fuels without central melting or high fission gas release. Post-irradiation measurements showed no evidence of fuel swelling or bowing as determined of the free-standing cladding. The high heat rating was found to be sufficient to produce some central void formation but nor for development of melting although columnar grain growth was significant. Data for columnar grain growth and equiaxed grain growth shown in Table 4.1 together with data from the earlier loop and poolside experiments can be compared with vi-pac UO_2-fuel rods where voids were formed at heat ratings for the integral $\int_{T_c}^{T_s} k d\theta$ of about 50 W/cm.

Effect of processing variables (calcining atmospheres and remote fabrication) on irradiation performance

Using different calcining atmospheres seemed to influence the fission gas release (Table 4.1, MTR III, ETR I). The fission gas release for NH_3 and Ar-4 % H_2 fired fuel was found less than 30 % whereas calcination in air occured about 40 % release. The comparison of UO_2 and Th/U-oxide vi-pac fuel indicated that thoria fuels can accomodate about 40 % higher heat ratings than urania without central melting at similar fission gas release rates and with nearly the same microstructural changes. Testing the effects of remotely fabricated rods containing ThO_2-3 % U-233 O_2-fuel showed that the rods perform well at linear heat ratings greater than 600 W/cm without incident (Table 4.1, ETR II) /54,91,107,110,111/.

Additionally, special irradiation test programs had been performed under the Light-Water Breeder Reactor program and in the Halden Boiling Heavy Water Reactor.

LWBR-irradiation program

Within the objective of the LWBR irradiation test program to determine irradiation induced structural changes, e.g. pellet densification, central void formation, grain growth and gas pore distribution as a function of thermal gradients, ThO_2-5,3 % UO_2-pellets (86,4 % th.D.), Zry-4-clad, were irradiated (about 4170 EFPH) to 1,5 x 10^{20} fiss/cm^3 in the L-12 loop of the ETR /113,114/. Because of the pellets low initial density, high temperatures were reached at the center. Extensive development of columnar grains as well

as central void formation occur in relatively short time (about 103 EFPH). The mechanism to explain segregation of alpha-emitting elements was found as a zone refinement process during void migration in a steep thermal gradient. In the L-12 loop of the ETR also ThO_2-20,01 % UO_2-pellets (80,6 % TD) were irradiated to 20 x 10^{20} fiss/cm^3 /95/. Fuel densification, columnar grains and a central void occured as a result of pore migration. Fission products as well as urania were depleted from the region of columnar grain to the outer periphery. The redistribution was related to lattice and grain-boundary diffusion under the influence of thermal gradients. In addition, Zr-4-clad fuel rods containing Th/U-oxide pellets (77,8 - 98,7 % TD, 2 - 24,7 % U-$235O_2$, 6,6 - 8,5 % U-$233O_2$) were irradiated from 70 - 750 W/cm reaching burnup levels up to 56.500 MWd/t (Th+U). Measured fission gas release was about 0,1 - 5,2 % increasing with higher temperature and higher burnups, whereas at higher initial density the release rate was found to be lower /96,97/.

Halden Boiling Heavy Water Reactor

Some experimental and operating experience with the Halden Boiling Heavy Water Reactor is available /115/. The study reported measurements on thermal conductivity for mixed ThO_2-UO_2 fuel and the effects of density and fuel to cladding gap on the center fuel temperature. The results also provided a considerable amount of information on diametral fuel expansion.

4.2.2 $(Th,U)O_2$-fuel element performance in power reactors

Light-Water Boiling Reactor BORAX IV

The performance of ThO_2- 6,36 % UO_2-pellets in X8001 aluminium alloy tube plates with silicon-bonded end closures was tested by irradiation in the BORAX IV reactor starting in 1957 /116/. Within the BORAX IV fuel testing, over one-third of the elements developed leaks during shut-down, caused by corrosion in cracks and crevices of a collapsed tubing. Although the pellets were irradiated at relatively low temperatures, they released about 3,4 % of the total fission gas yield by their open porosity. To get more irradiation performance data on Th/U-oxide pellet fuel /92,93/, two additional assemblies of ThO_2-pellets with different UO_2 compositions (6,36 %, 12,7 %, 25,6 %) were irradiated directly in the MTR-ETR process water at burnups about 33.200 MWd/t (Th+U), heat fluxes about 220 W/cm^2, peak linear heat ratings of about 300 W/cm, after an exposure time to reactor of 121 - 435 days releasing fission gas rates of 80 % in maximum. Two specimens failed by excessive internal pressure in areas of thin wall cladding caused by fuel thermal expansion and released fission gas (90 % of the

theoretical yield). The local cladding surface heat fluxes exceeded 265 W/cm^2. The characteristic central void formation developed at $\int_{T_0}^{T} k d\theta$ rating about 40 W/cm. Excess oxygen in the fuel is combined with lower thermal conductivity, considerable recrystallization and significant grain growth and fission gas release.

Light-water pressurized Indian Point Reactor

Performance of ThO_2-UO_2-fuel was furtheron demonstrated by irradiation in Indian Point Reactor /18,94,117-119/ starting in 1962. The stainless steel clad fuel pellets for Core A of the Consolidated Edison Indian Point Reactor were composed of highly enriched 0-9,1 % urania in thoria. Core A operated successfully 442 effective full-power days at burnup levels reaching 35.000 MWd/t (Th+U) and generating 2.8 billion kWh of electricity. In general the post-irradiation examination showed no major microstructural changes, diametral changes or ridging at pellet interfaces, no localized or general strains in the cladding, no areas of accelerated corrosion and no melting. The pellets were free to move within the tubing; fuel swelling and cracking were minimal. There was some movement of voids to the grain boundaries near the center and a considerable porosity on the inside surface of the cladding. In one sample U-235 was depleted to less than one-fourth of the initial amounts and in another the depletion was only about 15 %. Additionally, a series of loop and capsule in-pile tests for the Indian Point Reactor to study the irradiation effects on fabrication, design and materials to be utilized was performed in MTR-ETR process water. Specimens were irradiated at heat fluxes reaching 250 W/cm^2 and burnups of 20.000 MWd/t (Th+U) with little change exhibited on post-irradiation examination except for cracking /81/.

Heavy-water pressurized CANDU-reactor

Irradiation experience pertinent to CANDU-reactors was gained with $(Th,U)O_2$-fuel containing $\geq$ 10 % UO_2 on a limited range /19/. Within the irradiation test program using high-density fuel to compare the performance to UO_2, $(Th,U)O_2$-fuel elements containing 1,6 % UO_2 were irradiated successfully to burnups of about 400 MWh/kg (Th+U) at linear power outputs up to 650 W/cm. Fission gas release was about 1/10 of UO_2 while operating at the same power. Performance of $(Th,U)O_2$-fuel containing a defect in the cladding is even superior to that of UO_2. Fuel detorioration was much less, thus permitting such fuel to operate at higher power outputs for longer periods without significant physical degradation /84/. It was concluded, that redistribution of fuel

was probably of little concern in high density CANDU thorium cycle fuel whose centre temperature was limited to 2350K. If this centre temperature is exceeded or if the fuel contains substantial innerconnected porosity, the potential for redistribution is significant /72/.

4.2.3 $(Th,Pu)O_2$-fuel performance

The performance of "mixed-progeny"-fuel was demonstrated /54,78,91,105,107, 109,111,112/. Sphere-pac ThO_2 - 5 % PuO_2 fuel rods (Table 4.1 ETR IV-sphere-pac) were operated at heat ratings about 450 W/cm at burnup levels about 20.000 MWd/t (Th+Pu) and perform well, even in successful tests with 1000 W/cm. These high ratings discussed are only related to the material conditions, limitations under the aspect of reactor performance are not considered. Gross restructuring only occured in the center at highest heat ratings. Radial restructuring with central void formation was apparent. Microstructural changes were similar to those of UO_2-fuel under the same conditions. In comparing sphere-pac and pelletized fuel it was demonstrated that in slightly less than 20 days the sphere-pac fuel has begun to sinter developing a microstructure similar to that of pellets. As part of a study of crossed progeny fuel cycle, Zr-clad capsules containing $(Pu,Th)O_2$, high density pellets were irradiated under a variety of conditions to maximum burnups of about 3×10^{20} fiss/cm^3 at maximum power generation of over 1000 W/cm with central fuel temperatures above melting in the MTR/ETR. All capsules survived although the inner Zr-cladding failed on two of the high-power, high-burnup specimens. Structures developed were similar to those of UO_2 /120,121/. Columnar grain refinement occured with increasing linear heat ratings. Sintering and densification caused central void formation. Fission products migrated and were redistributed to the outer edge of columnar grain growth region during recrystallization and grain growth.

The performance of the ThO_2-PuO_2 (1,93 % PuO_2) irradiated in the NRX-reactor at linear heat ratings up to 77 W/cm and burnups of 1260 MWd/t (Th+Pu), compared well with that of UO_2 /122/, confirming previous observations that thoria is a more refractory material than UO_2 in terms of the rating required to effect a given structural change. Results demonstrated that irradiated Th/Pu-oxide pellets (1,1 - 2,7 % PuO_2) possess thermal conductivity higher than that of UO_2 and structural, dimensional changes and gas release should be less for a given power output /123,124/. Sintering studies, measurements of melting points, lattice parameters were performed in preparation for in-reactor evaluation /120,125,126/.

References

/1/ Panel Proceedings Series, "Sol-Gel Processes for Ceramic Nuclear Fuels", International Atomic Energy Agency, Vienna 1968

/2/ H. Lahr, "Fabrication and Properties of Particle Fuel", Kerntechnik 19. Jahrgang (1977) No. 4

/3/ P.A. Haas, K.J. Notz, R.D. Spence, "Application of Gel Microsphere Processes to Preparation of Sphere-Pac Nuclear Fuels", for presentation at the Ann. Meeting of Am. Cer. Soc., May 6 - 11, 1978, Detroit Michigan

/4/ L.R. Weissert, G. Schileo, "Fabrication of Thorium Fuel Elements", published by Am. Nucl. Soc., 1968

/5/ J.H. Handwerk, C.L. Hoenig, R.C. Lied, "Manufacture of the ThO_2-UO_2 Ceramic Fuel Pellets for BORAX IV", ANL-5678, Argonne National Laboratory, Aug. 1957

/6/ J.R. Fischer, E.D. Kendrick, "Comparison of Measured and Predicted Characteristics of the Elk River Reactor", Thorium Fuel Cycle Symp., Gatlinburg, 1966, pp. 681 - 694

/7/ E.S. Bomar, "Fabrication of ThO_2-$^{233}UO_2$ Pellets", ORNL-4820, Sept. 1972, pp. 154 - 155

/8/ J.E. McCauley, "Observations on the Irradiation Behavior of a Zr-4 Clad Rod Containing Low Density ThO_2-5,3 % UO_2 Pellets", WAPD-TM-664, Dec. 1969

/9/ T.J. Burke, "Planetary Ball Milling as a Method of Comminuting Presintered Thoria-Urania Granules", WAPD-TM-789, Apr. 1969

/10/ T.J. Burke, "Effect of Carbowax Binder and Dextrose Additive on the Microstructure, Density and Open Porosity of Thoria-Urania Fuel Pellets", WAPD-TM-880, Nov. 1969

/11/ W.A. Weinreich, W.H. Britton, C.R. Hutchinson, R.G.R. Johnson, T.J. Burke, "Fabrication of High-Density, High-Integrity Thoria-Base Fuel Pellets", Trans. Am. Nucl. Soc., 27: pp. 305 - 307 (1977)

/12/ Met. Div. Quar. Rep., Dec. 1956, ANL-5709, Argonne National Laboratory

/13/ P.D. Shalek, J.H. Handwerk, "Thoria-Urania Ceramic Fuel Bodies", ANL-5797, Argonne National Laboratory, Oct. 1958, pp. 9 - 11

/14/ P.D. Shalek, J.H. Handwerk, C.L. Hoenig, "Development of Ceramic Fuel Elements", ANL-5837, Argonne National Laboratory, Dec. 1957, pp. 11 - 15

/15/ E.D. Lynch, "Urania-Thoria Bodies", ANL-6330, Argonne National Laboratory, Ann. Rep. for 1960, pp. 90 - 93

/16/ H. Shapiro, R.M. Powers, "Thoria-Urania Pellet Preparation", Aug. 1959, SCNC-290

/17/ British Patent 1,241,976, "Process for Preparing Sintered Pellets of Ceramic Materials to be Used as Nuclear Fuel and Products Obtained by the Process", Aug. 1971

/18/ J.M. Kerr et al., "Indian Point I - A ThO_2-UO_2 Fueled Reactor", INKA-CONF-78-250-008

/19/ A.D. Lane, R.W. Jones, D. Hamel, "Fuel Technology for Denatured Thorium Cycles in CANDU Reactors", Trans. Am. Nucl. Soc. Vol 27, pp. 304 - 305, 1977

/20/ Thorium Fuel Cycle Dev., Stat. and Prog. Rep., Dec. 1963, compiled by R.G. Wymer and D.A. Douglas, Jr., ORNL-3611, pp. 102 - 108, 124 - 125

/21/ S.A. Rabin et al., "Irradiation Behavior of High Burnup ThO_2-4,45 % UO_2 Fuel rods", ORNL-3837, Oct. 1965

/22/ J.G. Stradley, J.M. Robbins, "Pelletizing of Sol-Gel Thoria-Urania Powders", ORNL-4170, Nov. 1967, pp. 219 - 220

/23/ J.D. Sease, A.L. Lotts, J.M. Robbins, "Bulk Oxide Process Development - Pelletizing", ORNL-4001, Oct. 1966, pp. 98 - 101

/24/ J.G. Stradley, J.M. Robbins, "Pelletizing", ORNL-4275, Jan. 1969, pp. 100 - 104

/25/ J.M. Robbins, J.G. Stradley, "Fabrication of Sol-Gel-Derived Thoria-Urania by Cold Pressing and Sintering", ORNL-4426, July 1969

/26/ R.L. Hammer, J.M. Robbins, R.A. Bradley, "Pelletizing of Sol-Gel Oxides", ORNL-4429, Aug. 1969, pp. 115 - 120

/27/ A.R. Olsen, J.D. Sease, R.B. Fitts, A.L. Lotts, "Fabrication and Irradiation Testing of Sol-Gel Fuels at Oak Ridge National Laboratory", ORNL-TM-1971, Sept. 1967, pp. 6 - 9

/28/ H.H. Crain, C.R. Hutchinson, "Fabrication of Fuel Pellets from Sol-Gel Powders", WAPD-TM-581 (Nov. 1966)

/29/ A. Liscia, S. Zanelli, "Fabrication of Sintered Pellets of Mixed Oxides of Th and U With Low Concentration of U for Fuel Elements", Atti Notiz. 26 No. 4, pp. 134 - 138 (Apr. 1971)

/30/ W.S. Ernst, Jr., R.L. Beatty, "Vibratory-Compaction Studies at the Oak Ridge National Laboratory", Symp. on Powder Packed Uranium Dioxide Fuel Elements, Nov. 30 - Dec. 1, 1961, CEND-153, Vol I, PP. 61 - 74

/31/ E.S. Bomar, W.S. Ernst, J.W. Snider, S.D. Clinton, P.A. Haas, A.W. Seifert, "Vibratory Compaction Studies", ORNL-3142, July 1961, pp. 22 - 27

/32/ W.S. Ernst, Jr., A.W. Seifert, "Vibratory Compaction Studies", ORNL-3160, Aug. 1961, pp. 60 - 61

/33/ W.S. Ernst, "Vibratory Compaction Research and Development", ORNL-3385, Oct. 1963, pp. 91 - 102

/34/ W.S. Ernst, Jr., "Vibratory-Compaction Studies", ORNL-3470, May 1963, pp. 204 - 205

/35/ W.S. Ernst, Jr., "Vibratory-Compaction Studies", ORNL-3870, Nov. 1965, pp. 281

/36/ W.S. Ernst, Jr., "Recent Vibratory-Compaction Studies on Thoria-Urania", Proc. of Thorium Fuel Cycle Symp., Gatlinburg, Tennessee, Dec. 5 - 7, 1962, TID-7650, Bk. 2 (July 1963), pp. 585 - 605

/37/ A.R. Olsen, S.A. Rabin, J.W. Snider, W.S. Ernst, J.W. Tackett, "Fabrication and Preirradiation Information on Vibratorily Compacted ThO_2-UO_2 Fuel Rods for Experiments ETR-I and MTR-III", ORNL-TM-1322, Jan. 1966

/38/ A.R. Olsen, J.D. Sease, R.B. Fitts, A.L. Lotts, "Fabrication and Irradiation Testing of Sol-Gel Fuels at Oak Ridge National Laboratory", ORNL-TM-1971, Sept. 1967, pp. 2 - 6

/39/ Div. of Reactor Dev., AEC Washington, D.C., "Nuclear Fuels and Materials Development", Sept. 1962, TID-11295, pp. 407 - 408

/40/ S.A. Rabin, M.F. Osborne, S.D. Clinton, J.W. Ullmann, "Thorium Fuel Cycle Irradiation Program at the Oak Ridge National Laboratory", Proc. of Thorium Fuel Cycle Symp., Gatlinburg, Tennessee, Dec. 5 - 7, 1962, TID-7650, Bk. 2 (July 1963), pp. 643 - 674

/41/ A.R. Olsen, R.B. Fitts, "Low-Energy Microsphere Packing (Sphere-Pac)", ORNL-4170, Nov. 1967, pp. 220

/42/ A.R. Olsen, "Vibratory-Compaction of Microspheres by the Sphere-Pac Technique", ORNL-4275, Jan. 1969, pp. 118 - 120

/43/ R.B. Fitts, A.R. Olsen, J. Komatsu, "Low-Energy Micorsphere Packing (Sphere-Pac)", ORNL-4429, Aug. 1969, pp. 109 - 115

/44/ A.R. Olsen, J.D. Sease, R.B. Fitts, A.L. Lotts, "Fabrication and Irradiation Testing of Sol-Gel Fuels at Oak Ridge National Laboratory", ORNL-TM-1971, Sept. 1967, pp. 12 - 15

/45/ R.R. Suchomel, "Progress on Sol-Gel Sphere-Pac Development", CONF-780535-1, Meeting Richland, WA, USA, 2 - 4 May, 1978

/46/ R.S. Miller, A. Liscia, "Extrusion Fabrication of Recycled Thoria-Urania in the PCUT Plant", Proc. of Thorium Fuel Cycle Symp., Gatlinburg, Tennessee, Dec. 5 - 7, 1962, TID-7650, Bk. 2 (July 1963), pp. 553 - 584

/47/ W.J. O'Leary, R.S. Miller, "Extrusion of UO_2 and ThO_2-UO_2 Nuclear Fuels", Symp. on Powder Packed Uranium Dioxide Fuel Elements, Nov. 30.-Dec. 1, 1961, CEND-153, Vol II, pp. 135 - 154

/48/ R.B. Fitts, J.D. Sease, "Sol-Gel Extrusion of Thoria-Base Ceramics", ORNL-4170, Nov. 1967, pp. 219

/49/ A.B. Meservey, K.H. Corkle, J.P. McBride, J.M. Robbins, J.G. Stradley, R.L. Hammer, R.B. Fitts, "Sol-Gel Extrusion", ORNL-4275, Jan. 1969, pp. 104 - 118

/50/ A.R. Olsen, J.D. Sease, R.B. Fitts, A.L. Lotts, "Fabrication and Irradiation Testing of Sol-Gel Fuels at Oak Ridge National Laboratory", ORNL-TM-1971, Sept. 1967, pp. 9 - 12

/51/ G. Cogliati, R. DeLeone, S. Ferrari, M. Gabaglio, "Extrusion of Mixed Oxide of Thorium and Uranium", VIII Nuclear Congress, Rome, 19 - 20 June, 1963, pp. 151 - 166

/52/ O.C. Dean, A.T. Kleinsteuber, J.W. Snider, C.C. Haws, P.A. Haas, "Sol-Gel Process Development", ORNL-3385, Oct. 1963, pp. 6 - 72

/53/ Chem. Techn. Division Ann. Prog. Rep., May 31, 1963, ORNL-3452, pp. 147 - 152

/54/ A.R. Olsen, D.A. Douglas, Y. Hirose, J.L. Scott, J.W. Ullmann, "Properties and Prospects of Thoria-Base Nuclear Fuels", ORNL-TM-1297, Nov. 1965

/55/ A.R. Olsen, J.D. Sease, R.B. Fitts, A.L. Lotts, "Fabrication and Irradiation Testing of Sol-Gel Fuels at Oak Ridge National Laboratory", ORNL-TM-1971, Sept. 1967, pp. 22 - 29

/56/ J.M. Pope, K.C. Radford, "Physical Properties of Some Thoria Powders and Their Influence on Sinterability", J. Nucl. Mater.; 52: No. 2, pp. 241 - 254 (Oct. 1974)

/57/ J.C. Clayton, "Thorium Oxide Powder Properties which are Important to ThO_2 and ThO_2-UO_2 Fuel Pellet Fabrication", WAPD-TM-1230, Jan. 1976

/58/ C.C. Busby, J.C. Clayton, "Thorium Oxide Granule and Compact Properties which are Important to ThO_2 and ThO_2-UO_2 Pellet Fabrication", WAPD-TM-1231, Jan. 1976

/59/ C.S. Morgan, L.L. Hall, A.R. Olsen, "Mechanical Properties of Sol-Gel Derived Fuel Bodies", ORNL-4429, Aug. 1969, pp. 132 - 136

/60/ M.J. Bannister, "Sintering and Grain Growth of Sol-Gel Thoria and Thoria-Urania", J.M. Robbins, "Sintering of Sol-Gel Oxides", ORNL-3870, Nov. 1965, pp. 281 - 282

/61/ M.J. Bannister, "Sintering and Grain Growth in Sol-Gel ThO_2 and ThO_2-UO_2", ORNL 4001, Oct. 1966, pp. 113 - 116

/62/ M. Mattys, R. Hauser, "Production de Pastilles d'Oxydes Mixtes UO_2-ThO_2 par Frittage dans l'Air", EUR 8.f, Mars 1962

/63/ A. Mohan, V.K. Moorthy, "Influence of Powder Characteristics on the Sintering Behavior of Oxide Mixtures", pp. 323 - 335 of High temp. mat. Bombay, 1972, see CONF-720223

/64/ A. Bassi, E. Brutto, G. Perona, G. Serem, R. Sesini, "Study and Observation of Sintering of Oxides of Uranium and Thorium", Energy Nucl. (Milan), 13: pp. 122 - 132 (March 1966)

/65/ R. Hauser, "New Developments Concerning the Technology of Uranium Oxide", pp. 519 - 528 of "Powder Met. in the Nucl. Age", Plansee Proc. 1961

/66/ R.J. Smid, "The Kinetics of Grain Growth in Thoria Pellets", Trans. Am. Nucl. Soc; 27: pp. 287 - 289 (1977), see WAPD-TM-1311, Jan. 1976

/67/ G.L. Spahr, "Densification Related Pellet Diameter Shrinkage in Low Burnup Thoria-Base Fuels", WAPD-TM-1345, Sept. 1978

/68/ R.W. Jones, H.R. Lee, H. Hahn, J.F. Walker, A. Celli, "Thoria Fuel Technology for CANDU-PHW Reactors", pp. 303 - 304

/69/ I. Cohen, "Effects of Thermal Gradients in Oxide Fuels", WAPD-TM-1092, March 1973

/70/ Thorium Fuel Cycle Dev., Stat. and Prog. Rep., Dec. 1963, compiled by R.G. Wymer and D.A. Douglas, Jr., ORNL-3611, pp. 117 - 124

/71/ D.N. Hess, B.A. Soldano, "Gas Evolution From Sol-Gel Uranium-Thorium Oxide Fuels", ORNL-4001, Oct. 1966, pp. 117 - 120

/72/ D.J. Cameron, "A Review of the Potential for Actinide Redistribution in CANDU Thorium Cycle Fuels", AECL-5962, Feb. 1978

/73/ R.M. Berman, "Methods for Assessing Homogeneity in ThO_2-UO_2 Fuels", WAPD-TM-1377, June 1978

/74/ A.R. Olsen, J.D. Sease, R.B. Fitts, A.L. Lotts, "Fabrication and Irradiation Testing of Sol-Gel Fuels at Oak Ridge National Laboratory", ORNL-TM-1971, Sept. 1967, pp. 18 - 22

/75/ C. Ferro, S. Moretti, C. Patimo, "Measurements of Thermal Diffusivity in Mixtures of the Oxides of Uranium and Thorium", BMBW-FBK-70-1, pp. 411 - 419

/76/ D.C. Jacobs, "In-Pile and Unirradiated Thermal Conductivity of a Single-Fired ThO_2 + 10 % UO_2", WAPD-TM-901, Feb. 1970

/77/ R.M. Berman, T.S. Tully, J. Belle, I. Goldberg, "The Thermal Conductivity of Polycrystalline Thoria and Thoria-Urania Solid Solutions", WAPD-TM-908, Dec. 1972

/78/ S.A. Rabin, "Irradiation Studies of Mixed Oxides of Thoria and Urania", ORNL-3385, Oct. 1963, pp. 102 - 128

/79/ R.E. Adams, S.A. Rabin, "Irradiation Studies", ORNL-3470, May 1963, pp. 205 - 208

/80/ Thorium Fuel Cycle Dev., Stat. and Prog. Rep., Dec. 1963, compiled by R.G. Wymer and D.A. Douglas, Jr., ORNL-3611, pp. 81 - 108

/81/ W.R. DeBoskey, "Irradiation Testing of Thoria Urania Fuel for the Indian Point Reactor", Proc. of Thorium Fuel Cycle Symp., Gatlinburg, Tennessee, Dec. 5 - 7, 1962, TID-7650, Bk. 2 (July 1963), pp. 630 - 642

/82/ J. Matolich, Jr., V.W. Storhok, "Thermal Diffusivity Measurements of Irradiated Oxide Fuels", BMI-X-10274, Feb. 1970

/83/ D.L. McElroy, J.P. Moore, P.H. Spindler, "Thermal Conductivity", ORNL-4429, Aug. 1969, pp. 121 - 132

/84/ Quart. Rep. No. 2, "Irradiation Performance of Thoria-Urania Fuel Materials", BAW 3376-2, Oct. - Dec. 1964

/85/ J.L. Scott, D.F. Toner, R.E. Adams, "Fuel Evaluation-Specimens of ThO_2 Containing 5 % UO_2", ORNL-3160, Aug. 1961, pp. 71

/86/ S.A. Rabin, "Fission-Gas Release Studies", ORNL-3385, Oct. 1963, pp. 121 - 126

/87/ R.E. Adams, "Neutron-Activation Experiments on Mixed Oxides Produced by the Sol-Gel Process", ORNL-3470, May 1963, pp. 205

/88/ Thorium Fuel Cycle Dev., Stat. and Prog. Rep., Dec. 1963, compiled by R.G. Wymer and D.A. Douglas, Jr., ORNL-3611, pp. 152 - 153

/89/ R.J. Smid, "Gas Release from Thoria-Base Oxide Fuel Pellets", WAPD-TM-850, April 1971

/90/ W.C. Thurber, "Compacted Powder Fuel Irradiation Studies at the Oak Ridge National Laboratory, Symp. on Powder Packed Uranium Dioxide Fuel Elements, Nov. 30. - Dec. 1, 1961, CEND-153, Vol II, pp. 39 - 65

/91/ A.R. Olsen, J.W. Ullman, Y. Hirose, E.J. Manthos, "Irradiation Studies", ORNL-3870, Nov. 1965, pp. 283 - 289

/92/ L.A. Neimark, J.H. Kittel, "The Irradiation of Aluminium Alloy-Clad Thoria-Urania Pellets", ANL-6538, June 1964

/93/ Div. of Reactor Dev., AEC Washington, D.C., "Nuclear Fuels and Materials Dev.", Sept. 1972, TID-11295, pp. 179 - 182

/94/ C.J. Baroch, E.N. Harbinson, A.V. Munim, "Examination of Stainless Steel-Clad ThO_2-UO_2 Fuel Rods and Zircaloy-2 Can After Operation for 442 EFPD in the Indian Point Reactor", BAW-3809-6, Aug. 1969

/95/ R.M. Berman, "Fission Product Distribution in Oxide Fuels", WAPD-TM-1236, Dec. 1976

/96/ I. Goldberg et al., "Fission Gas Release from ThO_2 and ThO_2-UO_2 Fuels", WAPD-TM-1350, Aug. 1978

/97/ I. Goldberg, G.L. Spahr, J.F. Giovengo, L.A. Waldman, "Fission Gas Release from ThO_2 and ThO_2-UO_2 Fuels", Trans. Am. Nucl. Soc., Vol. 27, pp. 308 - 310, 1977

/98/ M.C. Naik, A.R. Paul, U.N.G. Kaimal, M.D. Karkhanavala, "Effect of Burnup on Release of Xenon from Thoria", Radiat. Eff., 25: No. 2, pp. 73 - 77 (1975)

/99/ M.C. Naik, K.N.G. Kaimal, M.D. Karkhanavala, "^{133}Xe-Release from Irradiated Thoria Powders at Low Temperatures", BARC-601, 1972

/100/ M.C. Naik, K.N.G. Kaimal, M.D. Karkhanavala, "Post-Irradiation Thermal Release of 133 Xe from Sintered (ThO_2-0,1 % $^{233}UO_2$) Pellets", BARC-754, 1974

/101/ M.D. Karkhanavala, M.C. Naik, K.N.G. Kaimal, O.P. Chawla, "Kinetics of Release of Xenon from Sintered (ThO_2-0,1 % UO_2) Pellets", BARC-513, 1971

/102/ M.C. Naik, K.N.G. Kaimal, M.D. Karkhanavala, "Release of Xenon from Low Dose Irradiated Thoria Pellets", J. Nucl. Mater. v. 67 (3), pp. 239 - 243 (Aug. 1977)

/103/ R.B. Fitts, "Fission Gas Release from Ceramic Fuels", ORNL-3870, Nov. 1965, pp. 288 - 289

/104/ D.F. Toner, J.L. Scott, "Fission Gas Release", ORNL-3142, July 1961, pp. 22

/105/ A.R. Olsen, J.H. Coobs, J.W. Ullman, "Current Status of Irradiation Testing of Thorium Fuels at Oak Ridge National Laboratory", Thorium Fuel Cycle Symp, Gatlinburg, 1966, pp. 475 - 494

/106/ S.D. Clinton, "Fuel Cycle Irradiations", ORNL-TM-608, April 1963, pp. 45 - 46

/107/ A.R. Olsen, D.B. Trauger, W.O. Harms, R.E. Adams, D.A. Douglas, "Irradiation Behavior of Thorium-Uranium Alloys and Compounds", ORNL-TM-1142, June 1965

/108/ A.R. Olsen, J.D. Sease, R.B. Fitts, A.L. Lotts, "Fabrication and Irradiation Testing of Sol-Gel Fuels at Oak Ridge National Laboratory", ORNL-TM-1971, Sept. 1967, pp. 29 - 48

/109/ A.R. Olsen, "Irradiation of Thoria-Base Bulk Oxide Fuels", ORNL-4170, Nov. 1967, pp. 220 - 223

/110/ A.R. Olsen, J.W. Ullmann, E.J. Manthos, "Irradiation of Oxide Fuels", ORNL-4001, Oct. 1966, pp. 102 - 112

/111/ A.R. Olsen, R.B. Fitts, "Irradiation of Bulk Oxide Fuels", ORNL-4275, Jan. 1969, pp. 121 - 134

/112/ Stat. and Prog. Rep. for Thorium Fuel Cycle Dev., ORNL-4429, Aug. 1969, Compiled by R.G. Wymer and A.L. Lotts

/113/ J.E. McCauley, "Irradiation-Induced Structural Changes Obtained in ThO_2-UO_2 Fuel", Trans. Am. Nucl. Soc., 13: pp. 35 - 36, June - July 1970

/114/ J.E. McCauley, "Observations on the Irradiation Behavior of a Zircaloy-4 Clad Rod Containing Low Density ThO_2-5,3 % UO_2-Pellets", WAPD-TM-664, Dec. 1969

/115/ G. Kjaerheim, E. Rolstad, "In-Core Study of Fuel/Clad Interaction and Fuel Centre Temperature", HPR-107, Jan. 1969

/116/ C.F. Reinke, L.A. Neimark, R. Carlander, J.H. Kittel, "Metallurgical Evaluation of Failed BORAX-IV Fuel Elements", pp. 112, L.A. Neimark, R. Carlander, "Irradiation of X8001 Aluminium Alloy-Clad, Lead Bonded ThO_2-UO_2 Pellets", pp. 105 - 108, ANL-6330, Ann. Rep. for 1960

/117/ C.J. Baroch, W.N. Bishop, "Performance of ThO_2-UO_2 Fuel in Indian Point Reactor", Trans. Am. Nucl. Soc., 11, 1968, pp. 494, see CONF-681 101

/118/ H.M. Ferrari, R.J. Allio, "Fuel Element Experience in Pressurized-Water Reactores", Nucl. Appl., Vol. 2, Dec. 1966, pp. 492 - 498

/119/ W.N. Bishop et al., "Postirradiation Examination of Thoria-Urania Fuel Rods-Isotopic Analysis of the Fuel-Final Report", BAW-3809-7, Oct. 1969

/120/ M.D. Freshley, H.M. Mattys, "Irradiation of $(Th,Pu)O_2$", Thorium Fuel Cycle Symp., Gatlinburg, 1966, pp. 463 - 473

/121/ M.D. Freshley, H.M. Mattys, "ThO_2-PuO_2 Irradiation Studies", HW-83298, Nov. 1964, pp. 5.13 - 5.17

/122/ A.T. Jeffs, "Irradiation Behavior of Experimental Fuel Assemblies of UO_2-PuO_2 and ThO_2-PuO_2", AECL-2674, Feb. 1967

/123/ A.T. Jeffs, "Thermal Conductivity of ThO_2-PuO_2 Under Irradiation", AECL-3294, April 1969

/124/ J.R. Mac Ewan, A.S. Bain, M.J.F. Notley, "Irradiation Experience with Fuel for Power Reactors", A/CONF. 49/P-158, May 1971, pp. 239 - 256

/125/ J.R. McLaren, "The Sintering Behavior of PuO_2-ThO_2", AERE-M-1964, Jan. 1968

/126/ M.D. Freshley, H.M. Mattys, "Properties of Sintered ThO_2-PuO_2", HW-76300, pp. 2.6 - 2.8, Dec. 1962, HW-76559, pp. 11.6 - 11.9, Jan. 1963

Table 4.1:

Experiment - Test Group	Fuel Rod Identification	Number	Fuel - Type of Oxide (ThO_2-UO_2/ThO_2-PuO_2)	Particle Size	Fuel Density (smeared density %theoretical)	Fuel Rod Dimensions: length (cm)	outer diameter (mm)	wall thickness (mm)	Cladding Material	Cladding Temperature (°C)	Exposure Time to Reactor (EFPD-effective full power days)	Time Averaged Linear Heat Rating (W/cm)	Max. Instantaneous Linear Heat Rating (W/cm)	Max. Burnup (MWd/t Heavy Metal)	Fr-85 Release (%)	Heat Ratings for Various Microstructural Changes (W/cm) $T/C_{0.10}$	$U/T_{0.10}$	$U/C_{0.10}$	$T/C_{0.40}$	$U/C_{0.40}$
MTR-I	U1	43-59	arc-fused[1,g]	b	85.7	28.7	7.95	0.635	1	100	110.2	299	362	12300	2.4	32.8				
	U2	-60	" "	"	85.6	"	"	"	"	"	276.2	287	388	42100	7.2	33.7				
	U3	-61	" "	"	85.5	"	"	"	"	"	707.5	267	419	71000	6.4	31.6				
	U5	-62	sol-gel[E1,g]	"	87.0	"	"	"	"	"	110.2	341	426	14000	0.5	37.8				
	Z5	-63	" "	"	85.2	"	"	"	"	"	375.2	286	347	40200	13.2	32.8				
	Z7	-64	" "	"	85.5	"	"	"	"	"	691.1	311	507	81000	17.0	34.6				
	Z8	-65	" "	"		"	"	"	"	"	1107	303		120000	2.6	34.2				
	712	43-39	ThO_2+4.45%UO_2	c	93	11.43	7.95	0.635	1	100	905	420	652	119400	22.8	44.9				
	729	-40	" "	"	"	"	"	"	"	"	660	461		96000	12.4	48.2				
	730	-41	" "	"	"	"	"	"	"	"	497	270		37000		31.5				
	645	43-44	" "	"	"	"	"	"	"	"	406	294		50000		42.6				
DRR loop	L-1-A		sol-gel26[1,g]	d	85.2	54.61	11.68	0.381	1	260	29.6	381	389	1600	2.3	46.5				31.2
	L-1-B		" "	"	84.1	"	"	"	j	"	"	499	509	2100	-	57.0		54.2		35.4
	L-1-C		" "	"	84.1	"	"	"	"	"	"	410	418	1730	3.9	49.6				38.2
DRRpoolside	03-5		sol-gel0[1,f]	b	84.8	17.8	15.87	0.505	k	705	215.2	304	337	5220	18.3	58.5				38.5
	03-6		" "	"	85.5	"	"	"	"	540	"	275	297	4040	-	46.7				"
MTR-II		43-75	sol-gel5[1,g]	e	87.3	57.15	7.95	0.635	1	100	745	384		110000	30					
		-76	" "	"	87.8	"	"	"	"	"	746	423		120000	24					
MTR-III			4.5% UO_2[a]																	
		43-77-14	sol-gel35[g]	e	87.6	30.48	11.11	0.635	1	110	973	463		78500	42					
		43-77-9	" "	"	88.4	"	"	"	"	"	973	554		92000	26					
		43-78-17	" "	"	86-	"	"	"	"	"		820		96000[n]						
		43-78-5	" "	"	89	"	"	"	"	"		820		96000[n]						
		43-79-11	" "	"	"	"	"	"	"	"		820		96000[n]						
		43-79-7	" "	"	"	"	"	"	"	"		820		96000[n]						
ETR-I			5.02% UO_2[a]																	
	18	43-80	sol-gel35-1[g]	e	88.1	30.48	11.11	0.635	1	100	140.5	870	1050	20400	38.6	82.3	76.5	49.3	49.3	
	10	43-80	" 35-2	"	88.4	"	"	"	"	"	"	865	1044	20000	27.8	82.2	79.9	38.1	38.3	
	8	43-81	" 35-3	"	88.1	"	"	"	"	"	"	914	1103	22000	21.4	86.2	75.3	42.2	39.3	
ETR-II			3% U-233																	
		43-83	BNLsol-gel[g]	e	90	48	13	0.9	j	200		670		21500	-					
		-84	" "	"	"	"	"	"	"	"		450		28000	47					
		-85	" "	"	"	"	"	"	"	"		660		38500[n]						
		-86	" "	"	"	"	"	"	"	"		660		38500[n]						
		-87	" "	"	"	"	"	"	"	"		660		38500[n]						
		-88	" "	"	"	"	"	"	"	"		660		38500[n]						
ETR-IV			5% PuO_2																	
		43-106	sol-gel[h]		84	24	13	0.9	j	250		660[n]		15400[n]	3-13					
		-107	" "		"	"	"	"	"	272		985[n]		20200[n]	"					
		-108	" "		"	"	"	"	"	260		855[n]		19200[n]	"					
		-109	" "		"	"	"	"	"	272		985[n]		24000[n]	"					
		-110	" "		"	"	"	"	"	260		855[n]		19200[n]	"					
		-111	" "		"	"	"	"	"	250		660[n]		15400[n]	"					
ETR-sphere-pac			5% PuO_2																	
		43-99-2	sol-gel[h]		83.4	19	6.4	0.25	j	325		430		5000	13.2					
		43-99-4	" "		83.2	"	"	"	"	280		360		2900	3.3					
		43-100-2	" "		83.9	"	"	"	"	305		395		3950	9.9					
		43-100-4	" "		83.3	"	"	"	"	270		330		3000	1.6					
Pellet rods		43-43	4.5% UO_2[a]	c	91	11.43	7.95	0.635	1	100	1173	230		99000	7					
		43-45	" "	"	"	"	"	"	"	"	1189	270		119000	-					
		43-46	" "	"	"	"	"	"	"	"	1189	250		108000	20					
NRX-I		X1	sol-gelA[1,g]	b	87.0	27.9	7.95	0.635	1	100		116	138	13400	2.2	16.5				
		X8	" "	"	86.5	"	"	"	"	"		141	168	16360	2.8	18.8				
		03	sol-gel8[1,g]	"	86.5	"	"	"	"	"		135	162	15690	3.6	19.1				
		05	" "	"	86.2	"	"	"	"	"		125	148	14450	2.9	17.3				
		H3	" "	"	85.7	"	"	"	"	"		86	102	10500	1.6	13.8				
NRX-II		A1	arc-fused[1,g]	b	85.5	57.15	7.95	0.635	1	100		132	138	3170	3.5	18.0				
		A2	" "	"	85.7	"	"	"	"	"		178	188	4310	3.3	22.2				
		C3	sol-gel6[1,g]	"	85.3	"	"	"	"	"		200	211	4960	4.0	24.1				
		C4	" "	"	82.6	"	"	"	"	"		166	175	4160	-	21.0				
NRX-III		S1-6	sol-gel5[1,g]		88$_{Eq}$	99	7.95	0.635	1	100		278		23000						
		3 rods	5.2% PuO_2[f] sol-gel		74$_{\%}$	27.9	7.95	0.635	1	100		245		29000	5					

	Sol-gel A	Sol-gel B	Sol-gel C[a]	Sol-gel D[a]	Sol-gel E[a]	Arc Fused	Sol-gel S
Total Uranium, wt %	4.31	4.39	4.01	2.50	4.0	3.96	5.21
Uranium enrichment, %	93	93	93	93	93	93	93
Carbon, ppm	110	100	60	40	130	120	80
Nitrogen, ppm	22	21	55	29	31	1130	30
Iron, ppm	100	50	265	140	160	130	300
Silicon, ppm	600	500	<20	<10	<10	20	20
BET surface area (N_2), m^2/g	0.20	0.26	0.03	0.008	0.011	0.11	0.17
O/U ratio	2.0	2.0	2.03	2.02	2.02	2.01	2.01
Volatile matter released in vacuum at 1200°C, cc/g	0.125	0.151	0.055	0.012	0.027	0.24	0.284
Lattice parameter, Å	5.591	5.592	5.593	---	5.593	5.594	5.594
Crystallite size, Å	2400	1700	2200	---	---	---	1600
Particle density, g/cc[b]	9.94	9.92	9.76	9.97	9.92	10.11	10.0
Packed density, g/cc[c]	8.69	8.69	8.36	8.74	8.74	8.6	8.8

[a]Cooled in pure argon after calcination in hydrogen.

[b]Toluene intrusion, pycnometric method. Theoretical density: 10.04 g/cc

[c]NAVCO air vibrator, 1/25-in. piston; 5/16-in.-o.d. x 11-in. stainless steel tube.

Table 4.1: Summary of Properties of Uranium-Thorium Oxides Used in Fabrication of Irradiation Specimens

a) Uranium enriched in U-235 to 93 %

b) 60 % -10+16 mesh; 15 % -70+140 mesh; 25 % -200 mesh;

c) pellets

d) 60 % -6+16 mesh; 25 % -50+100 mesh; 15 % -200 mesh;

e) 60 % -6+16 mesh; 15 % -70+100 mesh; 25 % -200 mesh;

f) tamp-packed

g) vi-pac

h) sphere-pac

i) 304 stainless steel

j) Zircaloy-2

k) 304 Hasteloy stainless steel

l) although equiaxed grain growth was observed, the extent has not been clearly defined

m) heat ratings are time averaged values for the various intergrals: T_c is the central temperature limit, T_v is the limit of void formation, T_{cg} is the limit of columnar grain growth, and T_{eg} is the limit of descernible equiaxed grain growth.

n) estimated from exposure history

5. Review of direct pelletizing with ex-gel $(Th,U)O_2$-fuel and impact on the program

Within the formerly performed Th-program, the fuel rods have been manufactured using vibration-compaction technology. Consequently, no data about the pelletizing of ex-gel kernels are available from that program. KWU, however, has a large scale experience with the direct pelletizing of oxide-ceramic powders, and the requirements, to which the pressfit and sinterfit kernels have to satisfy, are well known.

The main powder/kernels characteristics are presented, and the evaluation of these data shows the way how to begin with the investigations on fuel manufacturing.

5.1 Pressfit powder properties

The required properties of the green pellets are:

- high mechanical strength
- good surface condition
- homogeneous spatial density distribution
- low residual stress

A high mechanical strength is necessary to allow an easy handling of the green pellets. Due to the requirements on the surface quality of the sintered pellets, good surface condition is requested. Additionally, the residual stresses inside of the green pellet, which can lead to the generation of surface damages during sintering and grinding, influence the surface quality. Hence, the residual stress of the green pellet has to be kept at a low level. At least, the spatial distribution of green density has to be rather homogeneous in order get a uniform shrinkage behavior of the pellets. These conditions lead to the following characteristics, which pressfit powder of spherical particles (kernels) should exhibit.

a) The kernels mechanical strength has to be low, i.e. the kernels should break even under a low pressure. Breaking of kernels during pressing has two effects:

   - it generates new-non-smooth surfaces which are necessary for a good each-to-other clamping of the kernels, this leads to a sufficient mechanical strength without the addition of binder material which is usual in ceramic powder metallurgical manufacturing,

- the filling-up of the spaces between the kernels or the kernel fractions is better, if the disintegration of the kernel under the pressing strain runs easily and is complete.

The requirements on homogeneous microstructure in the pellet also demand for an extensive kernel disintegration. Probably, the mechanical properties of the kernels arise during the calcination process. The calcination leads to the generation of cracks and pores, as it is known from other metallurgical experiences. Size and length of the cracks and pores are responsible for the fracture behavior during pressing.

b) The form and size of the kernels are important to reach a sufficient green density and a low residual stress. For the microscopic fracture processes during pressing, a more elliptoid form of the kernels is considered to be better than an ideally spherical form. For the same reason a small mean value of diameter and a large standard deviation of the diameter distribution is desirable.

Both, kernel form and size are fixed by the precipitation process, and not changed essentially by the following calcination. Hence, the precipitation parameters have to be adapted, too, to the optimized kernel properties.

c) Another important point is the flowability of the powder/kernels. It is important to guarantee a good transport and blending behavior and the uniform filling of the press. But for ex-gel kernels an excellent flowability is given anyhow by the spherical form and there seems to be no need to govern the fabrication process with respect to the flowability of the kernels.

5.2 Sinterfit powder properties

The quality of the sintered pellets depends widely on the properties of the green pellet, as described already in the foregoing chapter. Beyond that, only the content of non-ceramic additions to the kernels is considered to have an influence on the sintering behavior. A high content of PVA or other organic material lowers the green density which can be achieved by pressing. If the removal of these materials during sintering is not complete or is completed at a late stage of sintering, an inclusion in the gaseous form can happen and can prevent the sufficient densification during sintering. Even swelling phenomena during sintering are well known, if there is a high gas pressure in closed pores of the pellets.

The cracking of the organic material at elevated temperatures is combined with a strong reducing effect, which could change the thermodynamics of the mixed oxide, in first line of the UO_2-part of the fuel. But this is not yet investigated quantitatively. A high degree of removal of the non-ceramic components should be performed during calcination rather than during sintering. Thus, there are further requirements on the calcination step, which partly could be in opposite to the requirements for a good powder quality.

5.3 Summary

Summarizing the experiences from the kernel manufacture ex-gel and the pellet fabrication with direct pelletizing, the follcwing aspects for adaptation of the gel-process to the requirements of direct pelletizing have to be considered:

- The precipitation step is responsible for the kernel's properties: form and size distribution. These properties influence the green density, the mechanical strength and the residual stresses of the green pellets. Thus, the precipitation parameters have to be controlled.
- The precipitation possibly adjusts the crystallite size of the kernels which is part of the sintering activity and therefore important for the sinter densification of the pellets.
- The calcination process can create or destroy the specific surface area of the kernels, thereby influencing the sintering acitvity too.
- The calcination seems to be responsible for the fracture of the kernels during pressing, which is a quality characteristic for the pellet.
- The removal of non-ceramic components from the fuel kernels should be performed within the calcination step, too, which leads to further boundary conditions for the process. It is decisive whether a dewaxing step before sintering is necessary or not.

These are, for a first attempt, the main points to begin with the investigations on $(Th,U)O_2$-pellets. They should demonstrate the interdependencies and finally result in the final product -kernel, green, respectively sintered pellets- in a quantitative manner, and they should give basis for a specification of the process parameters in order to regulate these optimized properties.

6. Status report on Brazilian expertise on fabrication of fuel rods of the PWR type

6.1 Introduction

Brazilian expertise on fabrication of fuel rods of the PWR type is limited up to this moment to the fabrication of prototype rods for irradiation tests. Industrial experience will only be achieved after the erection of the fuel element plant at Resende - which will incorporate the KWU and RBU know-how.

The experience which has been gained up to now has evolved in the context of the Fuel Element Project, of the earlier Companhia Brasileira de Tecnologia Nuclear, CBTN - today succeeded by NUCLEBRAS - which intended to make a scale-up study on rod production - beginning by small rod fabrication, and then, gradually increasing their length, and inserting real components and parameters of a full-scale PWR fuel rod.

With the Brazil-Germany Nuclear Agreement, the Fuel Element Project which foresaw the fabrication in the country of complete fuel elements, from the experience acquired with prototypes, has been disactivated due to the technological package which has been acquired from Germany, and which includes the design and fabrication of fuel assemblies. There has remained, nevertheless, the experience on design and fabrication of small rods, which have been utilized in the irradiation programmes of the earlier Fuel Element Project.

For the fabrication of prototype rods, NUCLEBRAS starts from materials already worked out, part of which is acquired abroad, as is the case of Zircaloy tubes and rods and also UO_2 powder and pellets, and the other part of which is acquired in this country, such as the UO_2 pellets which are produced at the Instituto de Pesquisas Energéticas e Nucleares (Institute for Energética-cal and Nuclear Research) - IPEN - in Sao Paulo, Brazil, earlier - Instituto de Energia Atômica (Institute for Atomic Energy) - IEA - which has been working under contract for NUCLEBRAS to produce those pellets.

Next, summary comments about the methods and equipments utilized will be made, in order to get an idea of the presently settled production capacity, in this country, for PWR prototype fuel rods.

All methods and equipments which are described here are utilized at NUCLEBRAS-Centro de Desenvolvimento de Tecnologia Nuclear (Nuclear Technology Development Center) - CDTN, in Belo Horizonte and those referring to UO_2 pellets are utilized at IPEN, in Sao Paulo.

6.2 Methods and equipments

6.2.1 Zircaloy tubes and bars

Zircaloy tubes and bars are imported, obeying Specification Norms ASTM B353-71 and NUCLEBRAS Norms, and undergo a rigorous quality control, performed in CDTN laboratories, before being utilized in fuel rods.

Quality control tests are performed according to specifications adopted by NUCLEBRAS. Usually, the following tests are performed:

1 - Chemical Analysis

2 - Visual Examination

3 - Ultrasonic Inspection

4 - Metallographic Examination

5 - Mechanical Tests

6 - Corrosion Tests

7 - Dimensional Analysis

8 - Hydride Orientation and Texture Control

Figures 6.1, 6.2, 6.3, 6.4 and 6.5 show an overall view of the equipment used for some of the above mentioned quality control tests.

6.2.2 Uranium oxide (UO_2) Pellets

The nuclear fuel of uranium oxide, for the fabrication of the PWR prototype fuel rods, has been acquired by NUCLEBRAS from abroad, as pellets, or as powder, both enriched up to about 3.4 % of U^{235}.

In the last case, NUCLEBRAS has hired IPEN's work for the manufacturing of pellets from the imported powder. When utilizing natural uranium, IPEN fabricates under contract the pellets from ammonium diuranate (ADU), coming from NUCLEMON, a NUCLEBRAS subsidiary, and purified at IPEN itself.

It should be mentioned that IPEN has developed, in the course of many years research work towards the fabrication of UO_2 pellets, having however experience only with powder originating from the ADU process, noting that pellets coming from the AUC powder - which is the process utilized by RBU and has been bought by Brazil - still requires experimental work. IPEN ownes a well-equipped laboratory for the production of UO_2 pellets, besides a pilot plant for that purpose.

The laboratory as much as the pilot plant has as its starting material the ammonium diuranate. The pilot plant occupies an area of approximately (110 x 95) m^2, and has the following characteristics and equipments: a store room, a room of (5 x 2,5) m^2 for the diuranate control, an oil furnace for the calcination of the diuranate to U_3O_8, a room of (5 x 2,5) m^2 for the control of the U_3O_8 powder, a reduction furnace for U_3O_8 to UO_2 with a capacity of 2 kg of UO_2/hour, an equipped room, for the preparation of the mixture of the UO_2 powder with an agglomerative, and stove drying, a stokes precompactation press with a capacity of 240 pellets/min., a pellet granulator, a stokes dual action automatic press for the final compactation of the pellets, with a capacity of 45 pellets/min., and another press with floating die, a Harper sintering furnace with a Mo resistance and a working temperature of 1700°C, 30 KW power, with continuous running of molybdenum boat, with a capacity of 30 pellets/boat, and a total capacity of 2 kg of UO_2 pellets/hour, 3 centerless-grinder machines, one of which for primary grinding, and two series-connected, for the final grinding of the pellet. The pilot plant has an area for quality control, where the control of the powder and of the pellets are performed by international standards. The main equipments which compose the quality control area are a BET specific area measuring system, precision balances, pellet cutter a Fisher-Sieve sizer particle size measurer, a Rigaku portable X-ray diffraction equipment, and optical, quantitative, and electronic scanning and transmission microscopes besides a Talysurf for surface roughness measurements.

The laboratory has basically the same equipments as the pilot plant has, on a small scale of production and in lower degree of automation, whilst the quality control equipment and some for fabrication complement each other.

The fabrication of UO_2 pellets at IPEN generally is carried out according to the following scheme:

1. Receipt of the ammonium diuranate from the Chemical Engineering Center or from outside supplier.
2. Weighing and control of the diuranate and sending to calcination at about 550°C.
3. Weighing and control of U_3O_8 and sending to hydrogen reduction at 750°C.
4. Quality control tests of the UO_2 powder and mixing of the agglomerative and the lubricant and sending to compactation.

5. Sintering.

6. Grinding.

7. Dimension quality control, besides eventual control such as characterization, surface roughness measurement, etc.

IPEN's UO_2 pellet production sector evidently, is technically supported by other sectors as, for example, in the area of chemical analysis.

IPEN's Chemical Engineering Center has assembled, and operates, a pilot plant, the final objective of which is UF_6 production. At that plant, uranyl nitrate and ammonium diuranate of nuclear purity are obtained - that purity is attained through chemical reactions in pulsed column, from an uranium concentrate -. The uranium concentrate raw material is delivered to IPEN by NUCLEMON, a subsidiary of NUCLEBRAS. That Chem. Eng. Center has also assembled a pilot plant for the production of thorium nitrate of a nuclear purity from a thorium concentrate from NUCLEMON.

IPEN's Chemical Engineering Center has also worked at the fabrication of UO_2 and ThO_2 microspheres, utilizing the Hydrolysis process developed at KFA, and with the assictance of that center - which has donated a gel precipitation column -.

NUCLEBRAS, up to 1978, has worked in the area of ceramic fuel only in what concerns fuel design, performance predictions, irradiation tests and evaluation, having formed its staff in the context of the Fuel Element Project. The characterization and quality control of UO_2 pellets, was worked at CDTN laboratories. Part of the above mentioned design, testing, and evaluation group is, at present, working at CDTN, and the other part of it works at NUCLEBRAS Fuel Element Factory, being installed at Resende.

In 1979, in parallel to the installation of the Fuel Element Factory, NUCLEBRAS, aiming at the formation of a supporting group to the industrial sector and the development of researches in the field of fuel - for example on the development of optional fuels, such as mixed oxides - has planned a ceramic fuel laboratory, which is in phase of installation.

CDTN ceramic fuel laboratory is scheduled to start operation in 1980.

6.2.3 Machining and dimensional control of tubes and endplugs

Endplugs to be welded on the ends of the fuel rods are machined from Zircaloy-4 bars. using a common lathe, at CDTN workshop. Those plugs are numbered by a vibratory engraver, and controlled to their dimensions and internal and

external defects, before being welded to the rods. Dimensional control is made by utilizing a profile projector model Mitutoyo PJ 300 and micrometers and calipers. A metallographic examination is made to the internal flat surface of the plug to verify if there are any possible microchannels, resulting from the bar fabrication.

Tubes are cut to dimensions close to those in the utilization for the rod, using a diamond impregnated wire cutting system, or a lathe. Further, the tubes are just squared on their ends, in a common lathe, to the dimensions of the rods. The squaring of the tubes is generally performed at 90^{o}.

6.2.4 Cleaning of tubes and plugs

Zircaloy tubes and plugs, after an individual codification are controlled and stored and, undergo a "clinical" cleaning before being welded. A usual cleaning is made to the tubes and plugs by utilizing commercial acetone and sponge. A special cleaning can also be performed just before loading the UO_2 pellets into the fuel rod. For this is used an Ultrasound equipment specially for cleaning. The pieces are dipped into the container of the equipment, and kept under sound vibration during about 5 minutes in distilled water.

6.2.5 Welding of the first endplug to the tube

The welding of tube-endplug is a critical point, and therefore an intense research effort has been developed at CDTN in this field, which has resulted in the design and fabrication of a special equipment, which utilizes the TIG process (see Figure 6.6).

6.2.6 Quality control of the first weld

After the welding of the first endplug to the tube, several examinations are performed upon the weld, aiming at quality control. The following examinations are performed:

1. Leakage Examination

   This examination is performed by utilizing a Leybold - Heraeus helium leakage detector, model Ultra-Test M. The tube is evacuated through its open end, by the detector and helium is sprayed on the weld bead. If there is any leakage through the weld, this leakage is shown by the detector, which gives a quantitative measure of the leak. Leakage is admissible up to 1.10^{-8} Torr l/s. This examination is effected upon all welds. Figure 6.7 illustrates it.

2. Radiographic Examination

The radiographic examination is carried out upon the weld bead to detect porosities, internal deformation, lack of penetration and tungsten inclusions. All welds are X-ray examined. The X-ray technique, for this case, consists in utilizing a fine grain film (on the range of 1 - 100 μm) and a Zircaloy compensation block. The wall thickness of the compensation block, over the tube, varies from 0.5 to 2 mm, depending on the tube wall thickness. The equipment which is used in CDTN is a 300 KV Picker - Andrex. Usually, radiographs are taken from 2 angles: 0^{o} and 90^{o}. The most commonly detected defects are pores (admitted up to 0.25 mm), and lack of penetration. This last type of defect causes rejection of the weld. Figure 6.8 shows the equipment which is utilized.

3. Visual Inspection

This inspection is performed upon every weld, to detect surface flaws which might eventually occur on the weld bead. One utilizes, in this case, a magnification of 5 x, being however important to have it under adequate luminosity of the room (100 feet-candle).

4. Destructive Control

As a more rigid contol of the welds, and of the welding parameters and non-destructive procedures, one brings about destructive control upon a fraction of the welds which have been performed as test samples. The most important of the destructive controls is the metallographic one. The weld is cut off, polished, and then etched, for further observation in a microscope. Another destructive control which is carried out is the corrosion test in an autoclave. That test can reveal the presence of nitrogen in the weld, being a way of controlling the impurity of the welding environment. The presence of nitrogen is revealed through white spots. The autoclave temperature is about $350^{o}C$, and its pressure is of 168 atm.

6.2.7 Loading of the UO_2 pellets

UO_2 pellets, before being loaded into the rods, undergo a drying process, to remove adsorbed humidity. This is important, as the maximum humidity content in the fuel rod is limited to 10 ppm ($\sim$12 μl of hydrogen/g of UO_2). For drying of the UO_2 pellets, a stove is utilized. The drying temperature is of 140^{o} - $160^{o}C$, for 2 hours.

The loading of pellets has been made in a glovebox. This chamber is partly evacuated and filled with argon, thereby controlling the humidity of the environment. The handling of pellets and tubes in the interior is externally made, with the use of two rubber gloves fixed on the chamber wall. Meantime, another process has been tested, which consists of the following:

1. Drying of pellets in a stove.
2. Infrared drying tubes with first endplugs welded, (70°C) for some minutes, after cleaning with P.A. acetone.
3. Tube evacuating and filling with inert gas, inside the vacuum chamber. After being filled with inert gas, tube is closed, inside the chamber, with a teflon plug. This operation can be carried out in the welding chamber itself.
4. Pellet taking-off from the drying stove, and the introduction, as quickly as possible, into the rod tube, closed to the stove. Plugging with a teflon plug, and immediate carrying to the welding chamber. Taking-off of the teflon plug and introduction of the open end of the tube into the welding chamber.
5. Evacuation of the welding chamber, and filling with the inert gas. Welding of the second endplug without taking the rod off from the chamber.

6.2.8 Welding of the second endplug to the rod

The welding of the second plug to the rod is carried out just as that of the first, but without the gas inflow through the open end - which, in this case is already a closed one. There are two possibilities, as to the usage of the welding gas. If the rod is pressurized with helium at a high pressure (22 atm), the plug is already axially drilled, and the welding is carried out under argon, for a later pressurization and sealing with helium in another chamber. If the rod is filled with helium at a low pressure ($\sim$1.5 atm), the welding is performed directly under helium, and in this case the endplug is not drilled.

For the quality control of the second welding the following examinations are performed:

1. radiographic
2. visual
3. dimensional

All these examinations are performed in an identical manner as for the first welding.

6.2.9 Sealing of the second plug

The sealing of the second plug aims at introducing helium under pressure into the fuel rod. The sealing is carried out in a pressurization chamber, and the process which is utilized is the same TIG welding process. In the present case, however, the electrode lies in a horizontal position, and the second plug is axially drilled. After the evacuation of the chamber and the rod to 10^{-2} Torr and filling with helium, the arc is struck on the sealing orifice.

The duration of the arc is about 2 seconds with a current of about 60 A, which closes the orifice by melting. The sealing chamber was designed and built at CDTN, and may be used to pressurize rods under a helium pressure of up to 30 atm.

For the quality control of the sealing is used X-rays, for non - destructive control, and metallographic examination, for destructive control. The equipment and technique which are utilized are the same, already described, which are used in the welding of the endplug. Figure 6.6 shows the sealing chamber, connected to the welding system.

6.2.10 Rod quality control

After the sealing of the second plug, and the control of that sealing, the rod is still subjected to a rigid quality control, wherein the following examinations are performed:

1. Leakage Examination with Helium Leak Detector
2. Radiography to Check for Pellet Position Inside the Rod and Coarse Cracks.
3. Dimensional.
4. Weight.
5. Visual.

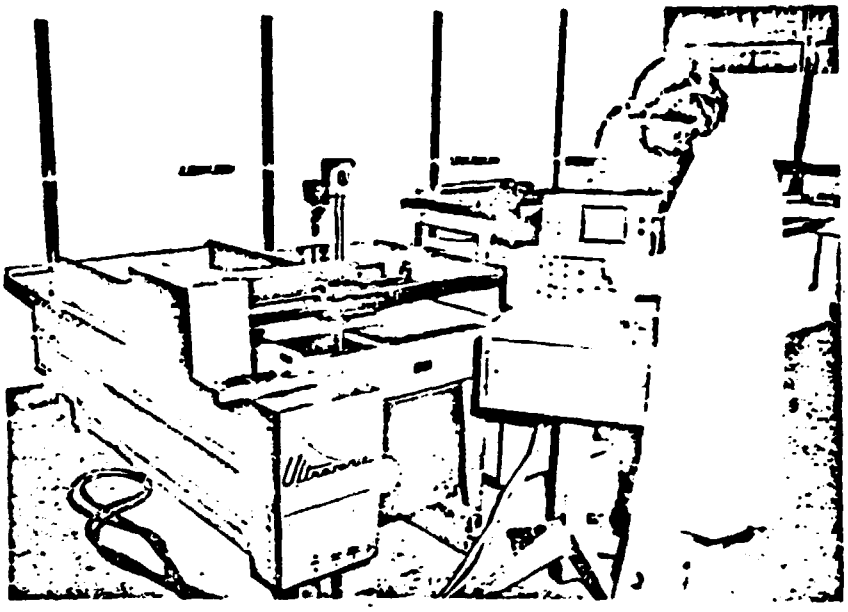

Fig. 6.1: Ultrasonic inspection of Zircaloy tubes

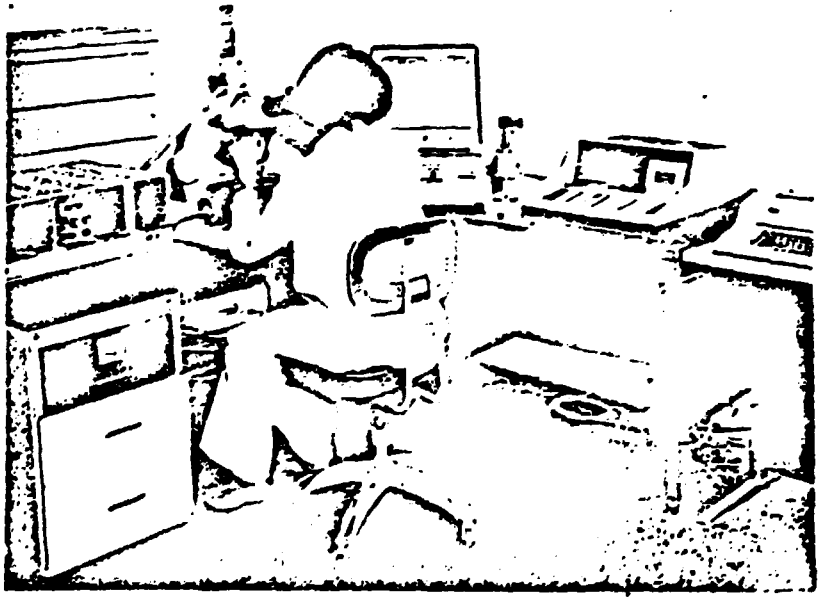

Fig. 6.2: Metallographic examination of Zircaloy and UO_2 pellets

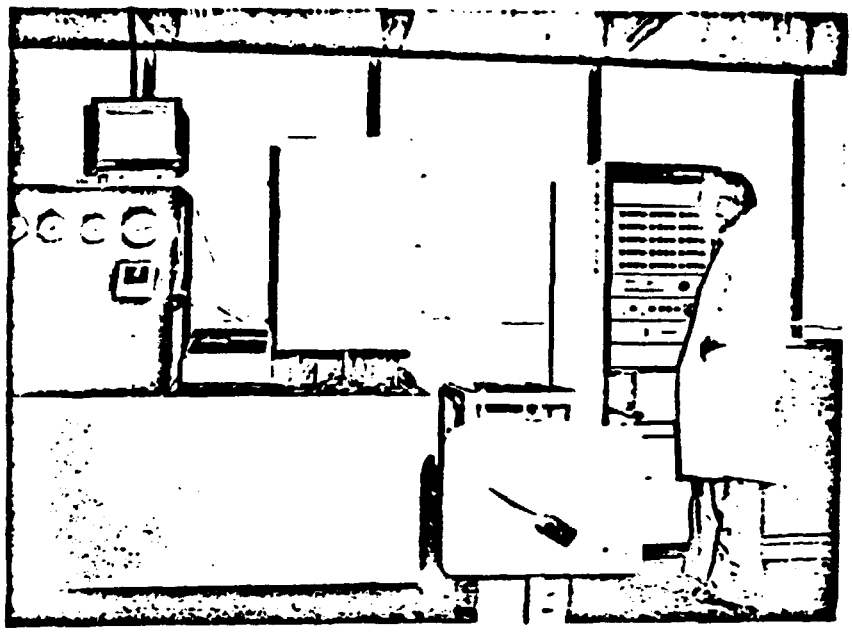

Fig. 6.3: Equipment for burst and creep tests used for Zircaloy quality control testing

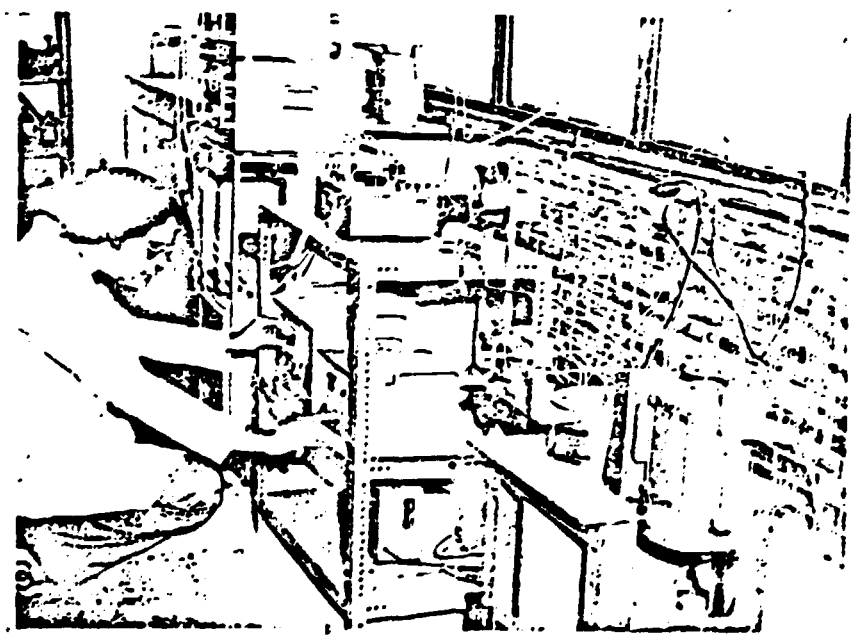

Fig. 6.4: Autoclave system for Zircaloy corrosion tests

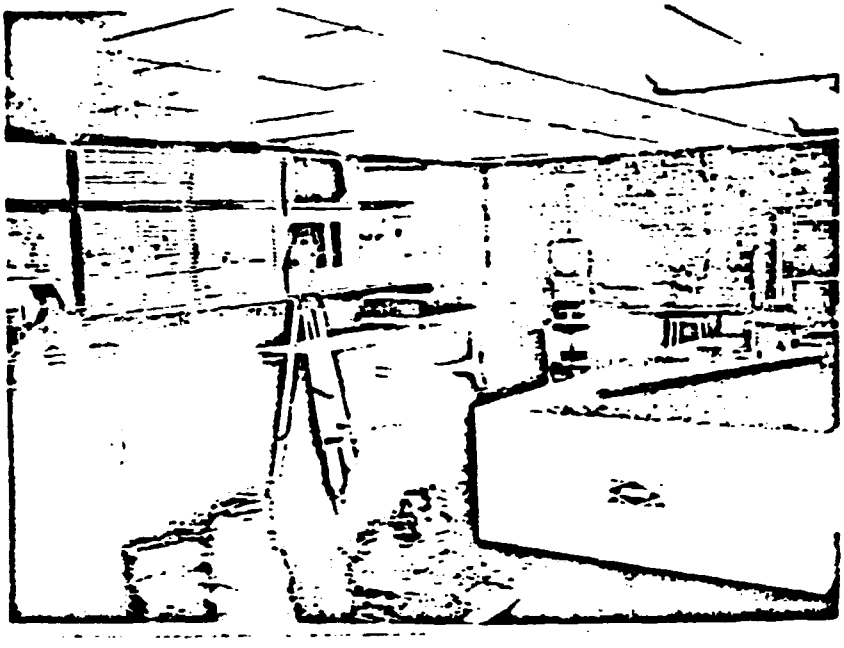

Fig. 6.5: View of the metrology laboratory used for dimensional analysis of fuel element components

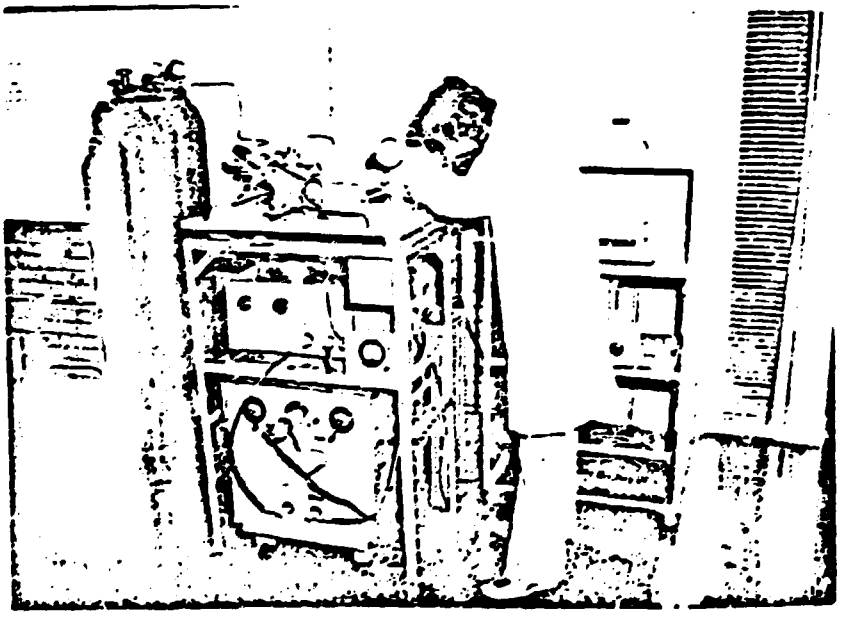

Fig. 6.6: Equipment with two chambers for welding Zircaloy tube-endplug, and sealing the fuel rod under high pressure helium

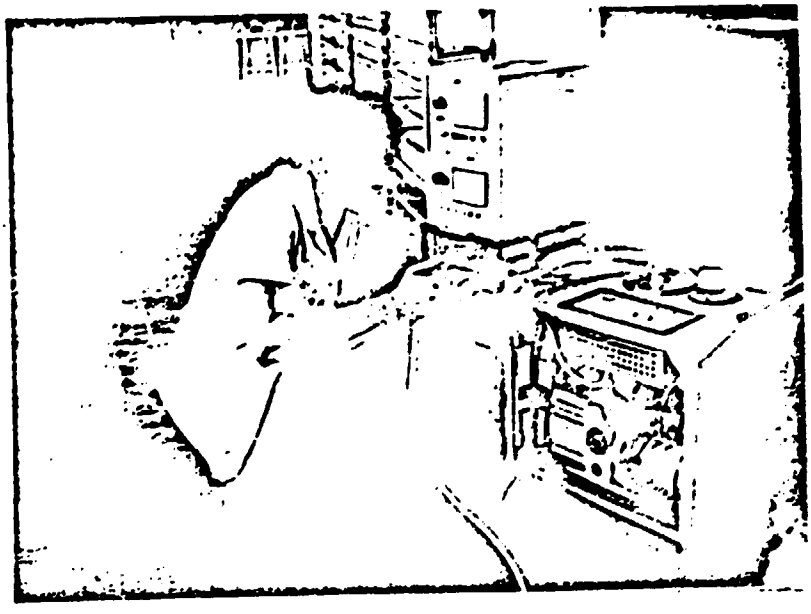

Fig. 6.7: Helium leak detection performed on welded fuel rod

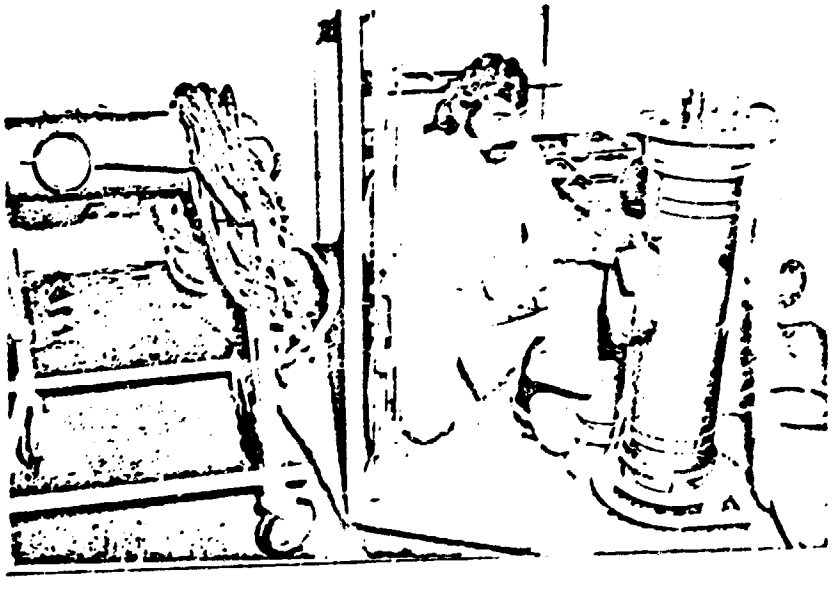

Fig. 6.8: X-ray equipment for weld examination